Journal of Medicinal Chemistry

Article

pubs.acs.org/jmc

Derivatives of Dibenzothiophene for Positron Emission Tomography Imaging of α7-Nicotinic Acetylcholine Receptors

Yongjun Gao,[†] Kenneth J. Kellar,[‡] Robert P. Yasuda,[‡] Thao Tran,[‡] Yingxian Xiao,[‡] Robert F. Dannals,[†] and Andrew G. Horti*[,†]

[†]Russell H. Morgan Department of Radiology and Radiological Sciences, Division of Nuclear Medicine, The Johns Hopkins University School of Medicine, 600 North Wolfe Street, Baltimore, Maryland 21287-0816, United States

[‡]Georgetown University, 3900 Reservoir Road, Washington, D.C. 20007, United States

ABSTRACT: A new series of derivatives of 3-(1,4-diazabicyclo[3.2.2]nonan-4-yl)dibenzo[*b*,*d*]thiophene 5,5-dioxide with high binding affinities and selectivity for α7-nicotinic acetylcholine receptors (α7-nAChRs) (K_i = 0.4−20 nM) has been synthesized for positron emission tomography (PET) imaging of α7-nAChRs. Two radiolabeled members of the series [^{18}F]**7a** (K_i = 0.4 nM) and [^{18}F]**7c** (K_i = 1.3 nM) were synthesized. [^{18}F]**7a** and [^{18}F]**7c** readily entered the mouse brain and specifically labeled α7-nAChRs. The α7-nAChR selective ligand **1** (SSR180711) blocked the binding of [^{18}F]**7a** in the mouse brain in a dose-dependent manner. The mouse blocking studies with non-α7-nAChR central nervous system drugs demonstrated that [^{18}F]**7a** is highly α7-nAChR selective. In agreement with its binding affinity the binding potential of [^{18}F]**7a** (BP_{ND} = 5.3−8.0) in control mice is superior to previous α7-nAChR PET radioligands. Thus, [^{18}F]**7a** displays excellent imaging properties in mice and has been chosen for further evaluation as a potential PET radioligand for imaging of α7-nAChR in non-human primates.

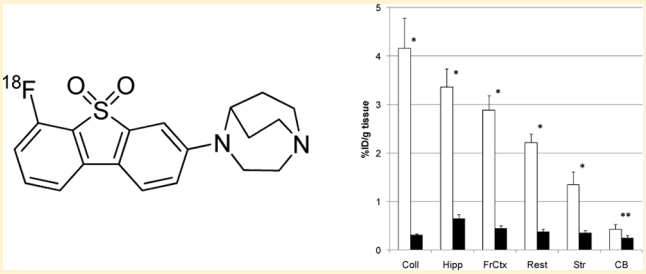

INTRODUCTION

Cerebral neuronal nicotinic cholinergic receptors (nAChRs) are ligand-gated ion channels composed of α (i.e., α2−α10) and β (i.e., β2−β4) subunits that can assemble in multiple combinations of pentameric structures. Among the many nAChRs subtypes in the human CNS, heteropentameric α4β2-nAChRs and homopentameric α7-nAChRs are predominant.[1,2] α7-nAChRs are composed of five identical α7 subunits, and each subunit provides an orthosteric binding site for its neurotransmitter acetylcholine.[3] Many lines of evidence associate α7-nAChRs with the pathophysiology of a variety of disorders such as schizophrenia and AD, anxiety, depression, traumatic brain injury, multiple sclerosis, inflammation, and drug addiction.[4−12]

Clinical experiments with α7-nAChR agonists have demonstrated that selective activation of the receptor is a viable approach toward improving cognitive performance in patients with schizophrenia.[13,14]

Because of the importance of the α7-nAChR in human neurophysiology and as a potential drug target, synthesis and preclinical examination of α7-nAChR subtype selective compounds receive substantial interest in industry and academia.[9,14] A number of α7-nAChR drugs are currently in various stages of the development for treatment of a variety of disorders including schizophrenia, AD, multiple sclerosis, depression, asthma, and type 2 diabetes.[15−17]

In vivo imaging and quantification of α7-nAChR binding in humans would provide a significant advance in the understanding of α7-nAChR-related CNS disorders and could also facilitate novel α7-nAChR drug development. Positron emission tomography (PET) is the most advanced technique to quantify neuronal receptors and their occupancy in vivo, and the development of a suitable PET radiotracer for α7-nAChRs would be of particular interest.

Many lead structures of α7-nAChR ligands have been identified within various structural classes. A number of these ligands have been radiolabeled for PET ([^{18}F], [^{11}C]) and single-photon emission computed tomography (SPECT) ([^{123}I]) (Table 1) and studied in mice, pigs, and non-human primates as potential α7-nAChR probes.[18−29] Most of these radioligands entered the animal brain but manifested relatively low specific binding (for review, see refs 30−32) and insufficient BP_{ND} values (BP_{ND} < 1) (Table 1). [^{11}C]CHIBA-1001 is the only α7-nAChR PET radioligand so far that has been studied in human subjects,[25] but it also exhibits low specific binding (Table 1).

Because of the exceptionally low concentration (B_{max}) of cerebral α7-nAChR binding sites in the human (5−15 fmol/mg protein)[33] and animal brain (1.5−12 fmol/mg tissue),[34,35] a PET radioligand with high specific brain uptake for this receptor subtype must exhibit very high binding affinity and selectivity, along with other important properties (e.g., lipophilicity, polar surface area, suitability for radiolabeling) in

Received: May 3, 2013

   dx.doi.org/10.1021/jm401184f | *J. Med. Chem.* XXXX, XXX, XXX−XXX

Table 1. In Vitro Properties and Binding Potential in Cortex (BP_{ND}) of the Previously Published PET/SPECT Radioligands for Imaging of α7-nAChR

Radioligand	α7-nAChR, K_i, nM	BP_{ND}[a]		References
		Mice	Monkey or pig	
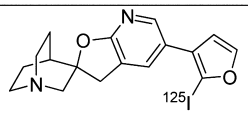	0.26	0.6	-	[18]
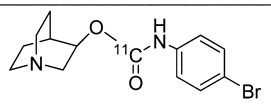	n/a	~ 0.3	-	[21]
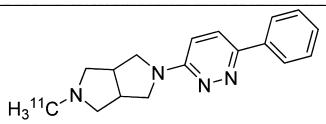 [^{11}C]A-582941	10.8	0.2 - 0.5	0.3	[22]
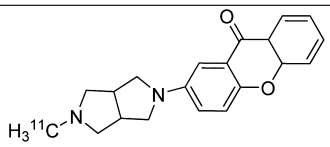 [^{11}C]A-844606	11	0.6 - 0.7	0.5	[22]
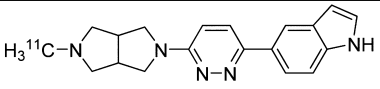 [^{11}C]A-833834	0.24, 1.53	0.5	-	[23]
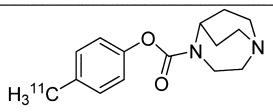 [^{11}C]CHIBA-1001	46, 120, 193	~ 0.6	0.6	[19, 25, 38, 39]
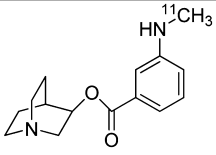 [^{11}C](*R*)-MeQAA	40.6	0.4	0.4	[20]
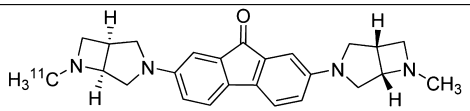 [^{11}C]A-752274	0.092	low brain uptake	low brain uptake	[23]
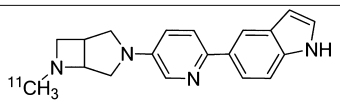 *rac*-[^{11}C]A-859261	0.5 - 0.6	1.9	-	[24]

dx.doi.org/10.1021/jm401184f | *J. Med. Chem.* XXXX, XXX, XXX–XXX

Table 1. continued

Radioligand	α7-nAChR, K_i, nM	BP_{ND}[a]		References
		Mice	Monkey or pig	
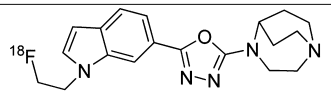 [^{18}F]NS14490	2.5	low brain uptake	-	28
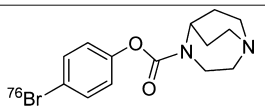 [^{76}Br]**1** ([^{76}Br]SSR180711)	24.9	-	0.7	19
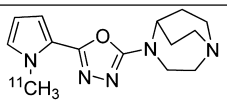 [^{11}C]**2** ([^{11}C]NS14492)	2.2	-	~ 1	26
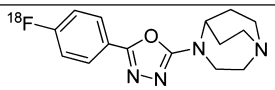 [^{18}F]**3** ([^{18}F]NS10743)	11.6	0.4	0.8	29
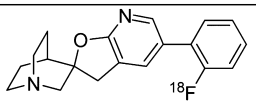 [^{18}F]**4** ([^{18}F]AZ11637326)	0.2	0.8	-	27, 40

[a]The BP_{ND} values in the cortex were taken directly from the corresponding references or estimated as $V_T/V_{ND} - 1$ or (cortex uptake/cerebellum uptake) − 1.[41,42]

an appropriate range (for details, see refs 30, 32, 36, 37). The general aptness of a PET radioligand for quantitative imaging studies is defined by a conventional criterion $B_{max}/K_D \geq 10$.[37] This equation predicts that a picomolar range of the binding affinity is required for a good α7-nAChR PET radioligand ($K_D \leq 0.15-1.2$ nM), whereas the most previously published α7-nAChR radioligands exhibited nanomolar binding affinities (Table 1). It is noteworthy, however, that the inhibition binding assays of the published compounds have been performed under a variety of assay conditions, and thus, the values of K_i listed in Table 1 may not be directly comparable to one another (see Results and Discussion for details).

Recently Abbott Laboratories has reported 3-(1,4-diazabicyclo[3.2.2]nonan-4-yl)dibenzo[*b*,*d*]thiophene 5,5-dioxide **5** (Figure 1) as an α7-nAChR selective antagonist with extraordinarily high binding affinity, K_i = 0.023 nM.[43] We

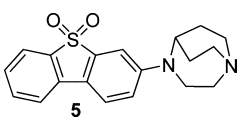

5

Figure 1. 3-(1,4-Diazabicyclo[3.2.2]nonan-4-yl)dibenzo[*b*,*d*]-thiophene 5,5-dioxide **5**, an α7-nAChR antagonist with very high binding affinity[43] that was used as the lead compound in this report.

envisioned the synthesis of fluoro derivatives of **5** producing a new set of compounds with similar or even better binding affinities with the potential for radiolabeling with [^{18}F] for PET imaging. The rationale for the design of fluorine-bearing analogues of compound **5** has been strengthened by reports that fluorine substituents can increase the metabolic stability and the rate and extent of blood−brain barrier penetration of radiotracers.[44]

In this study, we describe the design, synthesis and in vitro and in vivo characterization in mice of a series of high α7-nAChR binding affinity derivatives of **5** as potential probes for PET imaging of α7-nAChR receptor.

RESULTS AND DISCUSSION

Chemistry. *Synthesis of α7-nAChR Ligands.* The fluoro derivatives **7a−e** of 3-(1,4-diazabicyclo[3.2.2]nonan-4-yl)-dibenzo[*b*,*d*]thiophene 5,5-dioxide **5** were synthesized via the Buchwald−Hartwig cross-coupling reaction between the respective fluorobromo compounds **6a−e** with 1,4-diazabicyclo[3.2.2]nonane (Scheme 1).

The nitro derivatives of (1,4-diazabicyclo[3.2.2]nonan-4-yl)dibenzo[*b*,*d*]thiophene 5,5-dioxide **10** and **11** were synthesized similarly starting with respective nitrobromodibenzothiophene derivatives **8** and **9** (Scheme 2). Reduction of nitro groups in **10** and **11** with iron powder gave corresponding

dx.doi.org/10.1021/jm401184f | J. Med. Chem. XXXX, XXX, XXX−XXX

Scheme 1[a]

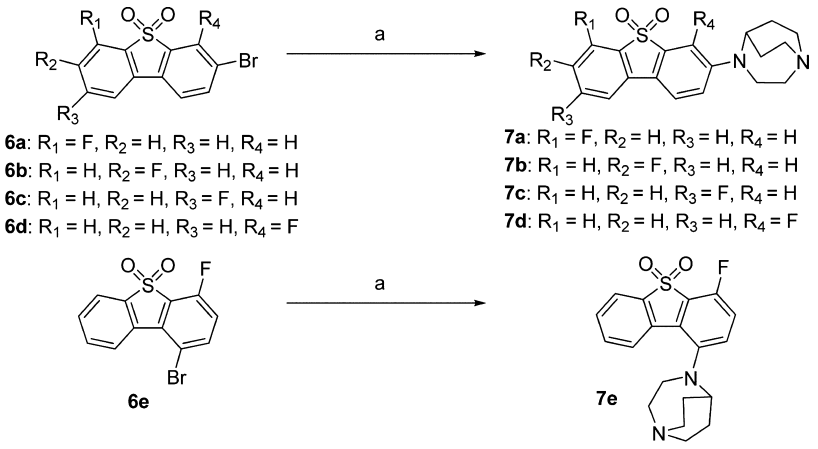

[a]Reagents and conditions: (a) $Pd_2(dba)_3$, *rac*-BINAP, toluene, 1,4-diazabicyclo[3.2.2]nonane, Cs_2CO_3, 85 °C, 24 h.

Scheme 2[a]

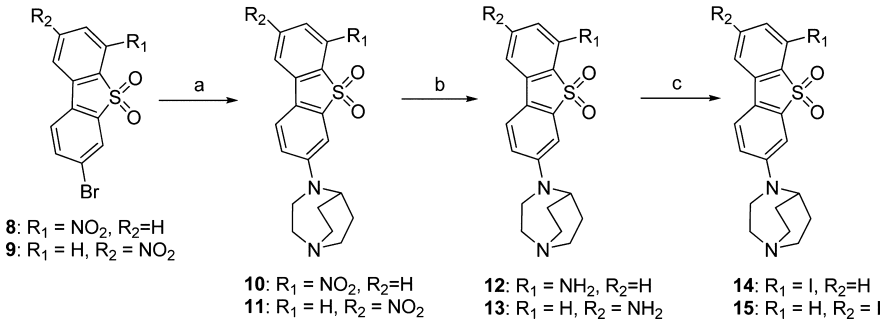

[a]Reagents and conditions: (a) $Pd_2(dba)_3$, *rac*-BINAP, toluene, 1,4-diazabicyclo[3.2.2]nonane, Cs_2CO_3, 85 °C, 24 h; (b) iron powder, NH_4Cl, THF, MeOH, water, 80 °C, 3 h; (c) (i) 4N H_2SO_4, CH_3CN, $NaNO_2$, −5 °C, 30 min; (ii) NaI, CuI, water 70 °C, 30 min.

Scheme 3[a]

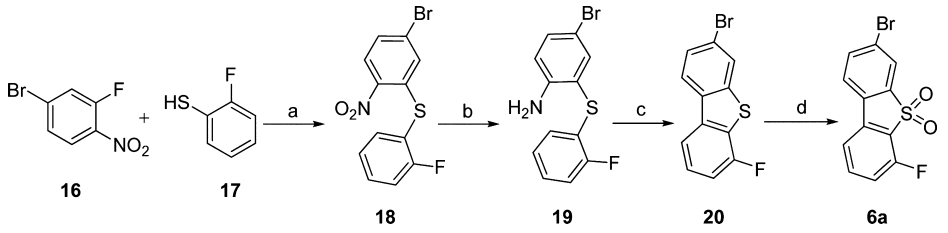

[a]Reagents and conditions: (a) Cs_2CO_3, DMF, 5 h; (b) iron powder, NH_4Cl, THF, MeOH, water, 80 °C, 3 h; (c) (i) $NaNO_2$, 37% HCl, 0−5 °C, 30 min; (ii) $NaBF_4$, 0−5 °C, 30 min; (iii) Cu_2O, 0.1 N H_2SO_4, 35−40 °C 30 min; (d) 30% H_2O_2, acetic acid, 60 °C, 24 h.

Scheme 4[a]

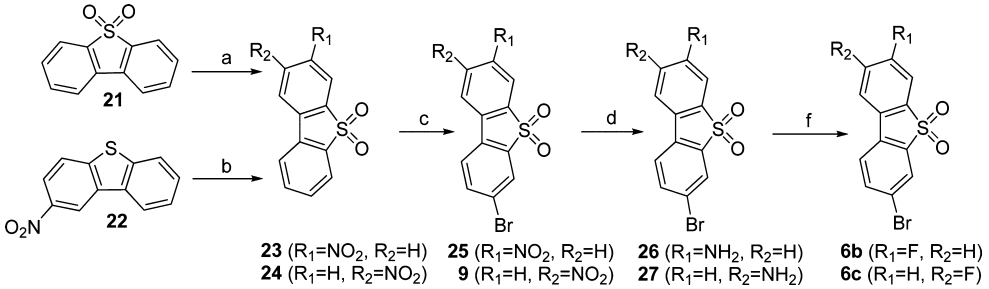

[a]Reagents and conditions: (a) H_2SO_4, HNO_3, 0 °C; (b) 30% H_2O_2, acetic acid, 60 °C, 24 h; (c) NBS, conc H_2SO_4 24 h; (d) $SnCl_2{\cdot}2H_2O$, 37% HCl, HOAc, 100 °C, 60 min or iron powder, NH_4Cl, THF, MeOH, water, 80 °C, 3 h; (f) (i) 48% HBF_4, 0−5 °C 10 min; (ii) $NaNO_2$, 0−5 °C, 1 h; (iii) xylene, 135 °C, 30 min.

dx.doi.org/10.1021/jm401184f | J. Med. Chem. XXXX, XXX, XXX−XXX

anilines **12** and **13** in high yield. Diazotization−iodination of **12** and **13** yielded corresponding iodides **14** and **15** (Scheme 2).

Synthesis of Intermediate Compounds. The synthesis of intermediate fluorobromide **6a** was performed in four steps (Scheme 3). Coupling of commercially available 4-bromo-2-fluoronitrobenzene **16** and 2-fluorothiophenol **17** gave nitrodiaryl thioether **18** that was reduced to aniline **19**. Aniline **19** was treated with sodium nitrite at 0 °C in the presence of hydrochloric acid and sodium tetrafluoroborate to yield a corresponding diazonium tetrafluoroborate derivative (not shown). The intramolecular deazotization/cyclization of the diazonium salt in the presence of copper(I) oxide and 0.1 N sulfuric acid afforded fluorobromodibenzothiophene derivative **20**, which in turn was oxidized with hydrogen peroxide to **6a** in high yield (Scheme 3).

The fluorobromo isomers **6b** and **6c** were synthesized in four steps via the commercially available dibenzo[*b*,*d*]thiophene 5,5-dioxide **21** and 2-nitrodibenzo[*b*,*d*]thiophene **22**, respectively (Scheme 4). In brief, nitration of compound **21** and oxidation of compound **22** gave compounds **23** and **24**, respectively. Bromination of compounds **23** and **24** provided monobromo derivatives **25** and **9** that sequentially were reduced to anilines **26** and **27**, respectively, in high yields. The anilines **26** and **27** were converted to fluorides **6b** and **6c** in moderate yields by the Schiemann reaction via the corresponding intermediate diazonium fluoroborates (structures not shown). The diazonium salts precipitated in the reaction mixture and were isolated by filtration in high yields.

The brominated isomers **6d** and **6e** were prepared by bromination of 4-fluorodibenzo[*b*,*d*]thiophene 5,5-dioxide **29** starting with 4-fluorodibenzo[*b*,*d*]thiophene **28** (Scheme 5).[45]

Scheme 5[a]

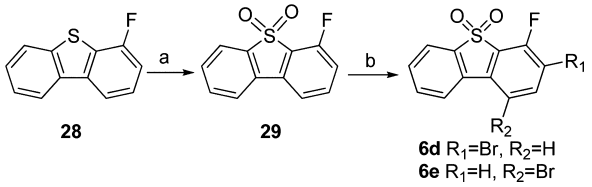

[a]Reagents and conditions: (a) 30% H_2O_2, acetic acid, 60 °C, 24 h; (b) NBS, H_2SO_4, 24 h.

Oxidation of **28** with hydrogen peroxide gave dioxide **29** in nearly quantitative yield. Bromination of **29** with 1 equiv of NBS in H_2SO_4 afforded two isomeric bromides: **6d** as the main product in 24% yield and **6e** as a minor product in 13% yield. A substantial amount of compound **29** (about 50%) was recovered from the reaction mixture. Isomers **6d** and **6e** were readily separated by silica gel chromatography.

3-Bromo-6-nitrodibenzo[*b*,*d*]thiophene 5,5-dioxide **8** was synthesized in two steps: (1) oxidation of 4-nitrodibenzo[*b*,*d*]-thiophene **30**[46] gave 4-nitrodibenzo[*b*,*d*]thiophene 5,5-dioxide **31** in 90% yield; (2) bromination of compound **31** provided compound **8** as the only product in 77% yield (Scheme 6).

In Vitro Inhibition Binding Assay. The results of the α7-nAChR in vitro inhibition binding assays for compounds **7a−e**, **10**, **11**, **14**, and **15** are shown in Table 2. In order to determine α7-nAChR selectivity of new compounds vs other nAChR subtypes, binding assays for the main cerebral heteromeric nAChR subtypes (α2β2, α2β4, α3β2, α3β4, α4β2, and α4β4) were also performed (Table 2). In addition, because α7-nAChR

Scheme 6[a]

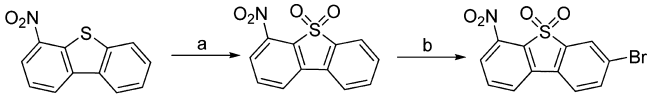

[a]Reagents and conditions: (a) 30% H_2O_2, acetic acid, 60 °C, 24 h; (b) NBS, H_2SO_4, 24 h.

shares 30% homology with the 5-HT_3 receptor and first generation α7-nAChR radioligands exhibited low α7-nAChR/5-HT_3 selectivity,[27] the in vitro binding affinity at the 5-HT_3 receptor was also determined for selected compounds of our series (Table 2).

α7-nAChR Assays. The α7-nAChR assays for **7a−e**, **10**, **11**, **14**, and **15** were performed using a commercial assay consisting of rat cortical membranes (rich in α7-nAChR) in competition against 0.1 nM [^{125}I]α-bungarotoxin, an α7-nAChR antagonist with a K_D of 0.7 nM. These assays were performed independently in duplicate, each twice (Table 2). Assays for two reference compounds, methyllycaconitine (MLA), a conventional reference α7-nAChR antagonist, and compound **5**,[43] a lead of our series, were also performed (Table 3).

The new series of fluoro isomers **7a−d** exhibited high binding affinity at α7-nAChRs with K_i values in the range 0.3−2.5 nM, whereas the binding affinity of isomer **7e** was lower (Table 2). The K_i values of the fluoro derivatives **7a−d** (Table 2) were better than that of the conventional reference α7-nAChR ligand MLA (Table 3). Among all fluoro isomers compound **7a** manifested the best α7-nAChR binding affinity that was an order of magnitude better than MLA and at least comparable to the nonfluorinated lead **5** (Tables 2 and 3).

Within the series **7a−e**, two fluoro derivatives **7a** and **7c** were selected for further evaluation. This selection was based on the high α7-nAChR binding affinity and selectivity of **7a** and **7c** (see Table 2) and the suitability of these compounds for radiolabeling with [^{18}F]. The radiolabeling of [^{18}F]**7a** and [^{18}F]**7c** was anticipated to be accomplished by a direct nucleophilic substitution (S_NAr) with [^{18}F]fluoride via the nitro **10** and **11** or iodo derivatives **14** and **15**, respectively. The leaving nitro groups in **10** and **11** or iodo groups in **14** and **15** are activated for S_NAr fluorination by the powerful electron-withdrawing SO_2Ar on the ortho and para positions, respectively.[47−50] We did not find in the literature an example of fluorination of nitro- or iododibenzothiophene 5,5-dioxides, but the structural analogue of **11**, 4,4′-sulfonylbis(*p*-nitrobenzene), has been converted to the corresponding fluoro derivative with good yield.[51]

The fluoro derivative **7b** that also exhibited high α7-nAChR binding affinity was not selected for further studies because the activating SO_2Ar was located on the meta position to the leaving group and direct radiolabeling of [^{18}F]**7b** via its nitro or iodo derivative was less likely. A detailed search of the literature for S_NAr reactions for 3-nitrodibenzo[*b*,*d*]thiophene 5,5-dioxide, a potential precursor for [^{18}F]**7b**, or its structural analogues (1-nitro-3-(phenylsulfonyl)benzene, etc.) did not reveal any previous publications.

The potential precursors **10**, **11**, **14**, and **15** for ^{18}F-fluorination of [^{18}F]**7a** and [^{18}F]**7c** were studied in the same α7-nAChR inhibition binding assay. The nitro compounds **10** and **11** exhibited α7-nAChR binding affinities comparable to

dx.doi.org/10.1021/jm401184f | J. Med. Chem. XXXX, XXX, XXX−XXX

Table 2. Inhibition in Vitro Binding Affinities (K_i, nM) of the New Series 7a–e, 10, 11, 14, and 15 toward α7-nAChR, Heteromeric nAChR Subtypes, and 5-HT$_3$

		heteromeric nAChR subtype[b]							selectivity	
compd	α7-nAChR[a]	α2β2	α2β4	α3β2	α3β4	α4β2	α4β4	5-HT$_3$[c]	α7/α4β2	α7/5HT$_3$
7a	0.37, 0.45	>10000	4000	1000	709	562	1000	230	1370	561
7b	1.02, 1.37	nt[d]	nt[d]	nt[d]	nt[d]	nt[d]	nt[d]	nt[d]		
7c	1.32, 1.35	1000	8000	2000	5000	885	3000	505	663	378
7d	1.83, 2.45	292	838	678	3000	141	1000	nt[d]	66	
7e	17.8, 20.3	>10000	562	2000	261	4000	251	nt[d]	210	
10	0.34, 0.35	nt[d]	nt[d]	nt[d]	nt[d]	nt[d]	nt[d]	nt[d]		
11	3.41, 6.21	nt[d]	nt[d]	nt[d]	nt[d]	nt[d]	nt[d]	nt[d]		
14	0.93, 1.93	nt[d]	nt[d]	nt[d]	nt[d]	nt[d]	nt[d]	nt[d]		
15	6.46, 8.77	784	6000	1000	9000	477	5000	nt[d]	63	

[a]Rat cortical membranes, radiotracer [^{125}I]α-bungarotoxin (0.1 nM). K_D = 0.7 nM. [b]Inhibition in vitro binding assay of all heteromeric nAChR subtypes was performed with stably transfected HEK293 cells and [^{3}H]epibatidine (0.5 nM). K_D = 0.021 nM (α2β2-nAChR). K_D = 0.084 nM (α2β4-nAChR). K_D = 0.034 nM (α3β2-nAChR). K_D = 0.29 nM (α3β4-nAChR). K_D = 0.046 nM (α4β2-nAChR). K_D = 0.094 nM (α4β4-nAChR).[55] [c]Human 5-HT$_3$ recombinant/HEK293 cells, radiotracer [^{3}H]GR65630 (0.35 nM). K_D = 0.5 nM [d]nt = not tested.

Table 3. Inhibition in Vitro Binding Affinities (K_i, nM) of Reference Compounds toward α7-nAChR[a]

compd	α7-nAChR
MLA	2.91 ± 0.76 (n = 9)
2	20.4
3	38.0
4	3.3
5	0.30, 0.50

[a]The binding assay conditions are the same as those in Table 2.

those of the corresponding fluorides **7a** and **7c**, whereas the binding affinities of iodo derivatives **14** and **15** were lower.

Currently, there is no conventional in vitro competition binding assay for α7-nAChR. Different research groups use different radioligands ([^{125}I]α-bungarotoxin, [^{3}H]α-bungarotoxin, [^{3}H]MLA, [^{125}I]iodo-MLA, [^{3}H]A-585539, etc.) and different sources of receptor tissue (cell lines, brain, adrenal glands) under different conditions for this assay.[26,29,52−54] It is not surprising that the difference in the K_i values for the same compound under different assay conditions can exceed an order of magnitude.[53,54] Therefore, a direct comparison of K_i values of the previously published α7-nAChR ligands with compounds of our new series is not practical.

For the purpose of comparison, we determined the K_i values of the three most recently published α7-nAChR PET radioligands [^{11}C]**2**,[26] [^{18}F]**3**,[29] and [^{18}F]**4**[27] (Table 3) under the same assay conditions as those of our series (Table 2). It was noteworthy that the α7-nAChR binding affinities of the best compounds of our series **7a** and **7c** were substantially better than those of the previous radioligands.

Heteromeric nAChR Subtypes Assays. The heteromeric nAChR subtypes assays (α2β2-, α2β4-, α3β2-, α3β4-, α4β2-, α4β4-nAChR) were performed in our laboratories using membrane preparations from HEK293 cells expressing the transfected nAChR under test in competition with 0.5 nM [^{3}H]epibatidine to investigate the specificity of the ligand for each receptor (Table 2).

The heteromeric nAChR K_i values of the tested compounds **7a**, **7c–e**, and **15** were substantially greater than the corresponding α7-nAChR K_i values, indicating a high α7-/heteromeric-nAChR subtype selectivity of all studied compounds (Table 2). Thus, the fluoro isomer **7a** with the best α7-nAChR binding affinity also manifested an excellent selectivity versus heteromeric nAChR including the main cerebral subtype α4β2-nAChR (Table 2). Interestingly, the α7/α4β2 selectivity of iodo derivative **15** is 10 times lower than the corresponding fluoro derivative **7c**.

5-HT$_3$ Assay. The in vitro binding affinity of the most promising members of the series, compounds **7a** and **7c**, at the 5-HT$_3$ receptor was determined commercially using membrane preparations from HEK293 cells expressing transfected human 5-HT$_3$R in competition with 0.35 nM [^{3}H]GR65630, a 5-HT$_3$R antagonist with a K_D of 0.5 nM. The assay demonstrated that fluoro compounds **7a** and **7c** manifest relatively low 5-HT$_3$ binding affinities and they are highly α7-nAChR/5HT$_3$ selective (Table 2).

Lipophilicity of 7a and 7c. Lipophilicity (log $D_{7.4}$) is considered an important property of CNS radioligand because it has been linked to the blood–brain barrier permeability and nonspecific binding.[35,37,38] The lipophilicity values for **7a** and **7c** (log $D_{7.4}$ = 2.0) were calculated with ACD Labs Structure Designer Suite (ACD Labs, Toronto, Canada) and fall within the conventional range for CNS PET radioligands.

Radiochemistry. We radiolabeled the fluoro isomers **7a** and **7c** that exhibited the highest binding affinity within the series with fluorine-18. The radiosyntheses were performed remotely in one step by 1,10-diaza-4,7,13,16,21,24-hexaoxabicyclo[8.8.8]hexacosane (Kryptofix-222) assisted radiofluorination of the respective nitro precursors **10** and **11** (Scheme 7) or iodo precursors **14** and **15** using a radiochemistry synthesis module (Microlab, GE) followed by the semipreparative HPLC separation and formulation of [^{18}F]**7a** and [^{18}F]**7c** as sterile apyrogenic solutions in 7% ethanolic saline.

Scheme 7. Radiosynthesis of [^{18}F]7a and [^{18}F]7c

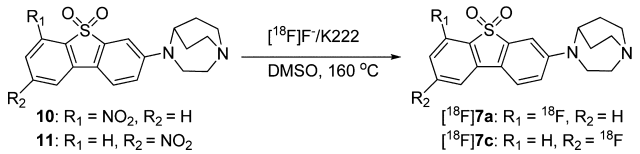

It is noteworthy that the radiotracer product yields from iodo precursors **14** and **15** were substantially lower than those of the nitro precursors **10** and **11**. The conventional Kryptofix-222/potassium carbonate assisted radiofluorination of both iodo

dx.doi.org/10.1021/jm401184f | J. Med. Chem. XXXX, XXX, XXX–XXX

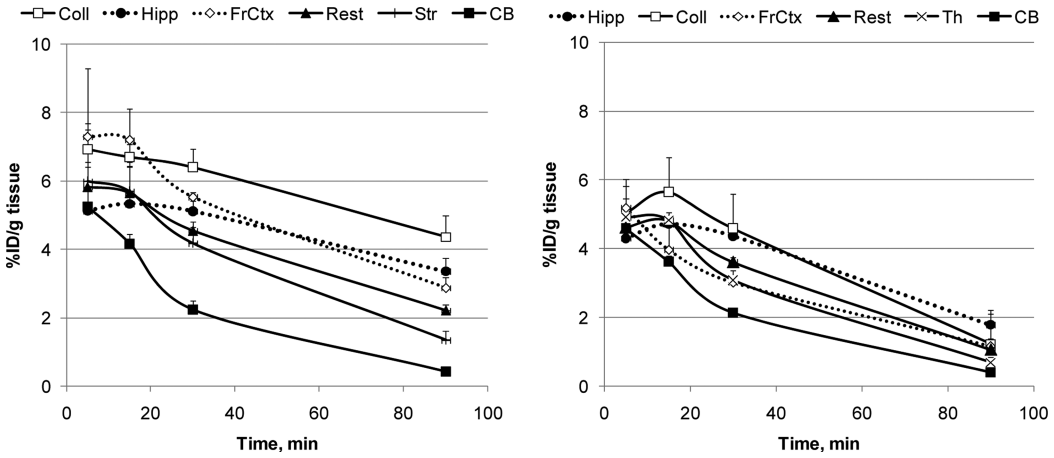

Figure 2. Regional distribution of [^{18}F]**7a** (left) and [^{18}F]**7c** (right) in CD-1 mice. Data: mean % injected dose/g tissue ± SD (n = 3). Abbreviations: Coll, superior and inferior colliculus; Hipp, hippocampus; FrCtx, frontal cortex; Rest, rest of brain; Th, thalamus; Str, striatum; CB, cerebellum.

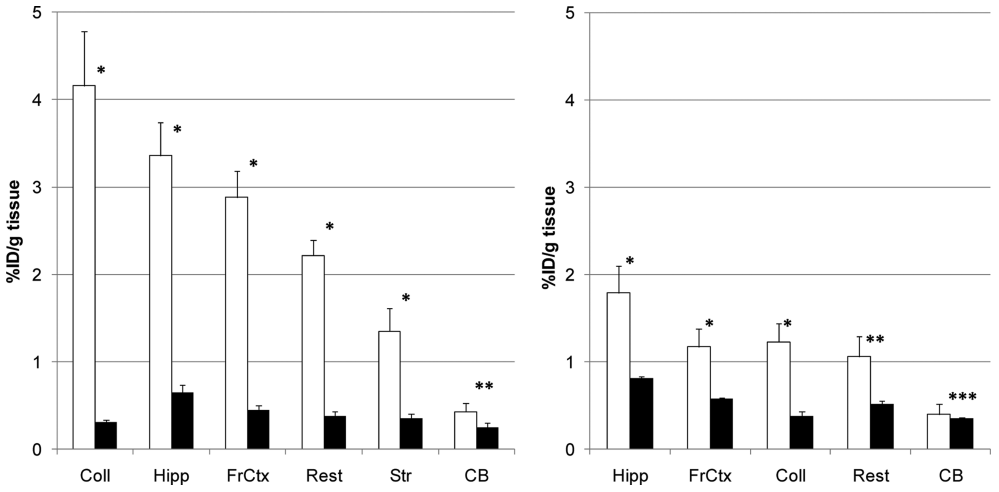

Figure 3. Self-blockade study of [^{18}F]**7a** and [^{18}F]**7c** in CD-1 mice. Left: Inhibition of [^{18}F]**7a** (0.07 mCi, specific radioactivity of 9200 mCi/μmol, iv) accumulation by intravenous co-injection with **7a** (0 mg/kg (white) and 0.3 mg/kg (black)) in the mouse brain regions 90 min after the injection: (*) $P < 0.01$, significantly different from controls; (**) $P = 0.04$, insignificantly different from controls (ANOVA). Right: Inhibition of [^{18}F]**7c** (0.07 mCi, specific radioactivity of 12 000 mCi/μmol, iv) accumulation by intravenous co-injection with **7c** (0 mg/kg (white) and 0.2 mg/kg (black)) in the mouse brain regions 90 min after the injection: (*) $P \leq 0.01$, (**) $P = 0.015$, significantly different from controls; (***) $P = 0.5$, insignificantly different from controls (ANOVA). Data are the mean % injected dose/g tissue ± SD (n = 3). Abbreviations: Coll, superior and inferior colliculus; Hipp, hippocampus; FrCtx, frontal cortex; Str, striatum; Rest, rest of brain, CB, cerebellum.

derivatives **14** and **15** in DMSO at 130−180 °C produced [^{18}F]**7a** and [^{18}F]**7c** with radiochemical yields below 0.5%, and this radiosynthesis pathway was not optimized further (not shown).

The radiofluorination of nitro derivative **10** or **11** (Scheme 7) in the presence of Kryptofix-222/potassium carbonate at 160 °C produced [^{18}F]**7a** or [^{18}F]**7c** in a slightly better yield (2−3%). Further optimization of this radiosynthesis suggested that both final products [^{18}F]**7a** and [^{18}F]**7c** rapidly decomposed in the DMSO reaction solution in the presence of highly basic K_2CO_3, but the radiochemical yield was improved if the less basic potassium oxalate was used. In the presence of potassium oxalate, the final products [^{18}F]**7a** and [^{18}F]**7c** were prepared under similar reaction conditions with comparable radiochemical yields of 16 ± 6% (n = 14) (nondecay-corrected), with specific radioactivities in the range 330−1260 GBq/μmol (9−34 Ci/μmol) and a radiochemical purity greater than 99%. The nitro precursors **10** and **11** that exhibited substantial α7-nAChR binding affinity (Table 2) were fully separated by preparative HPLC and were not detected by analytical HPLC in the final products [^{18}F]**7a** and [^{18}F]**7c** (see Table 6 for the HPLC details).

Biodistribution Studies of [^{18}F]7a and [^{18}F]7c in Mice. *Baseline Studies in Mice.* Radioligands [^{18}F]**7a** and [^{18}F]**7c** were evaluated in mice as potential PET tracers for imaging α7-nAChRs. After intravenous injection, [^{18}F]**7a** and [^{18}F]**7c** exhibited robust initial brain uptake followed by washout. The highest accumulation of radioactivity of both radioligands occurred in the superior/inferior colliculus, hippocampus, and frontal cortex. Moderate uptake was observed in thalamus and striatum, and the lowest radioactivity was seen in cerebellum (Figures 2−4). This distribution of radioactivity was similar to the previously published in vitro data on the distribution of α7-nAChRs in rodents.[56,57] The clearance rate of [^{18}F]**7a** and [^{18}F]**7c** from cerebellum was higher than that from any other region studied. The ratios of tissues to cerebellum increased steadily over the 90 min, reaching values of 10 for [^{18}F]**7a** and 4.5 for

dx.doi.org/10.1021/jm401184f | J. Med. Chem. XXXX, XXX, XXX−XXX

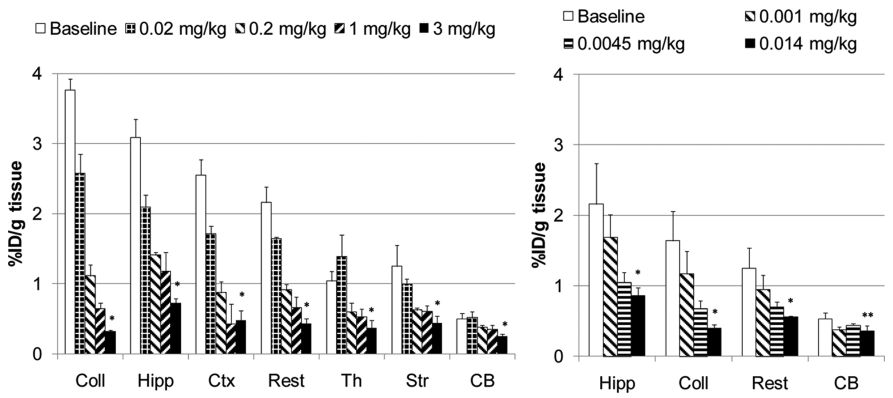

Figure 4. Blocking of [^{18}F]**7a** and [^{18}F]**7c** with α7-nAChR-selective ligands in CD-1 mice. Left: Dose dependent blockade of [^{18}F]**7a** (0.07 mCi, specific radioactivity of 7900 mCi/μmol, iv) accumulation by intravenous coinjection with **1** (doses 0.02, 0.2, 1, 3 mg/kg) in the mouse brain regions 90 min after the injection: (*) $P \leq 0.01$, significantly different from controls (ANOVA). Right: Dose dependent blockade of [^{18}F]**7c** (0.07 mCi, specific radioactivity of 11 000 mCi/μmol, iv) accumulation by intravenous co-injection with **5** (doses 0.001, 0.0045, 0.014 mg/kg) in the mouse brain regions 90 min after the injection: (*) $P < 0.01$, significantly different from controls; (**) $P = 0.06$, insignificantly different from control (ANOVA). Data are the mean % injected dose/g tissue ± SD ($n = 3$). Abbreviations: Coll, superior and inferior colliculus; Hipp, hippocampus; Ctx, cortex; Str, striatum; Th, thalamus; Rest, rest of brain; CB, cerebellum.

[^{18}F]**7c**. The better ratios for [^{18}F]**7a** vs [^{18}F]**7c** are in agreement with in vitro α7-nAChR binding affinity of these compounds (Table 2).

*Specificity and Selectivity of [^{18}F]**7a** and [^{18}F]**7c** Binding in the Mouse Brain.* A conventional in vivo blockade methodology with CNS drugs is used here for demonstration of specificity and selectivity at the α7-nAChR receptor in the mouse brain. A self-blockade study with a nonradioactive form of a radioligand estimates whether or not the binding is specific. A blockade study with a drug that is highly selective at the target binding site is expected to show the selectivity and specificity of the radioligand binding. A dose-escalation blockade with such a target selective drug provides further evidence of the radioligand specificity and selectivity, and it is useful for demonstration of the radioligand suitability for evaluation of conventional drug candidates. In addition, blockade with CNS drugs that do not bind at the target site provides more evidence of the radioligand selectivity versus other cerebral binding sites.

Self-Blockade Studies. Self-blockade studies of [^{18}F]**7a** with **7a** (Figure 3, left) and of [^{18}F]**7c** with **7c** (Figure 3, right) demonstrated a reduction of the radioligand uptake in most brain regions except the cerebellum, a region with low density of α7-nAChRs. The studies showed that accumulation of [^{18}F]**7a** and [^{18}F]**7c** radioactivity in the mouse brain was specific. When the specific binding of the radioligands in the hippocampus and colliculus was estimated by using the radioactivity concentration in the blocked cerebellum as nonspecific binding, the specific binding value amounted to 94% and 80% and the baseline-to-blockade ratio in the α7-nAChR-rich regions was 13 and 5 for [^{18}F]**7a** and [^{18}F]**7c**, respectively. This result also demonstrated that [^{18}F]**7a** exhibited a higher level of specificity and greater uptake in the mouse brain versus [^{18}F]**7c**.

Neither behavioral nor locomotor activity changes were observed in the mice in the blockade studies with **7a** (0.3 mg/kg, iv) or **7c** (0.2 mg/kg, iv).

Blocking with Selective α7-nAChR Ligands. A blockade study of [^{18}F]**7a** with **1**, a selective α7-nAChR partial agonist with a K_i of 22 nM,[58] showed a dose dependent blockade in all regions studied. However, in the α7-nAChR-poor cerebellum, the blockade was significant only with the highest dose of **1** (3 mg/kg) (Figure 4, left). A similar dose–response study was performed with [^{18}F]**7c** using compound **5**, a selective α7-nAChR antagonist, as a blocker (Figure 4, right). These studies confirmed that the in vivo binding of [^{18}F]**7a** and [^{18}F]**7c** was specific and mediated by α7-nAChR. The dose-escalation response demonstrated that both radioligands are suitable tools for evaluation of new α7-nAChR drug candidates.

It is noteworthy that the doses of **1** that significantly blocked the [^{18}F]**7a** binding in CD1 mice were comparable to the doses of **1** that significantly improved cognitive deficit in the various rodent models of schizophrenia.[59,60] This finding suggests that [^{18}F]**7a** is a suitable radioprobe for in vivo studies in mice with pharmacologically relevant doses of α7-nAChR drugs.

Because the lowest regional uptake of [^{18}F]**7a** and [^{18}F]**7c** was seen in the cerebellum, the regional BP_{ND} values in mice were approximated for a single time point measurement (90 min) as BP_{ND} = (regional uptake/cerebellum uptake) − 1 [42] (Table 4). The substantially higher BP_{ND} values for [^{18}F]**7a** are in agreement with greater binding affinity of this compound versus [^{18}F]**7c** (Table 2; also see Figure 7). The BP_{ND} values for both radioligands [^{18}F]**7a** and [^{18}F]**7c** were superior to all previously published α7-nAChR PET radioligands (Table 1).

Table 4. Approximate BP_{ND} Values (Unitless) of [^{18}F]7a and [^{18}F]7c in the Mouse Brain Regions[a]

	region		
compd	Coll	Hipp	Ctx
[^{18}F]**7a**	8.0 ± 1.6	5.5 ± 1.7	5.3 ± 1.2
[^{18}F]**7c**	2.0 ± 0.5	3.1 ± 0.7	2.0 ± 0.3

[a]Data: mean ± SD ($n = 6$). Abbreviations: Coll, superior and inferior colliculus; Hipp, hippocampus; Ctx, cortex.

Blocking with Nicotine and $\alpha4\beta2$-nAChR Selective Cytisine. The blockade of [^{18}F]**7a** in CD1 mouse brain with cytisine, a partial nicotinic agonist selective for $\alpha4\beta2$-nAChR and other $\beta2/\beta4$-containing heteromeric nAChR subtypes while exhibiting low α7-nAChR binding affinity,[52,55,61] showed insignificant reduction of radioactivity accumulation in all regions studied (Figure 5). This result demonstrated that [^{18}F]

dx.doi.org/10.1021/jm401184f | J. Med. Chem. XXXX, XXX, XXX–XXX

7a manifested insignificant binding at α4β2-nAChRs in the mouse brain.

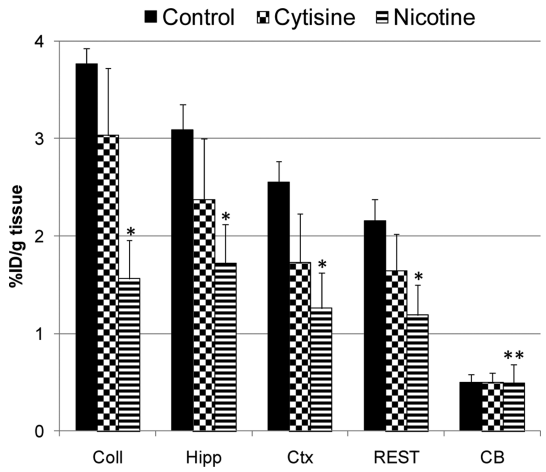

Figure 5. Blockade of [^{18}F]**7a** accumulation in CD-1 mouse brain regions by injection of cytisine (1 mg/kg, sc) and nicotine (5 mg/kg, sc) (both 90 min after the injection). Data are the mean % injected dose/g tissue ± SD (n = 3). Abbreviations: Coll, superior and inferior colliculus; Hipp, hippocampus; Ctx, cortex; CB, cerebellum; Rest, rest of brain. The effect of cytisine was insignificant in all regions studied (P > 0.05, asterisk is not shown). The difference between control and nicotine was significant ((∗) $P \leq 0.01$) in all regions except CB ((∗∗) P = 0.9) (ANOVA). The study demonstrates that [^{18}F]**7a** does not bind in vivo at the main cerebral α4β2-nAChR subtype and it is suitable for nicotine blockade studies.

The blockade study of [^{18}F]**7a** with nicotine that binds at all nAChR subtypes including α7-nAChR[52] showed significant blockade in all regions except the nAChR-poor cerebellum. This study suggests that [^{18}F]**7a** can be used for nicotine addiction or smoking studies in mice. The lesser blockade of [^{18}F]**7a** with nicotine (Figure 5) in comparison with **1** (Figure 4) is due to the rather modest binding affinity of nicotine at α7-nAChR (K_i = 610 nM).[52]

Blocking with Non-α7-nAChR CNS Ligands. For determination of in vivo selectivity of [^{18}F]**7a** for α7-nAChRs vs several major CNS receptor systems, we compared the regional distribution (Figure 6) of the radiotracer in control CD-1 mice vs mice preinjected with various CNS active drugs or the positive control **1** (see Table 5 for the drug list). None of the drugs except **1** reduced accumulation of radioactivity when compared with controls (Figure 6). The absence of blockade with the 5-HT$_3$-selective drug ondansetron was especially remarkable because α7-nAChR ligands often bind to this receptor subtype. This finding suggests that in the mouse brain the radioligand [^{18}F]**7a** was selective for α7-nAChRs versus several major cerebral binding sites.

Comparison of Imaging Properties of [^{18}F]7a and [^{18}F]7c with Previous α7-nAChR PET Radioligands. Binding potential (BP_{ND}), a measure of in vivo specific binding and one of the most important imaging characteristics of a PET radioligand, is defined as the ratio of B_{max} (receptor density) to K_D (radioligand equilibrium dissociation constant) or the product of B_{max} and binding affinity.[41,62] Therefore, the binding affinities ($1/K_i$) of α7-nAChR radioligands should correlate linearly with their BP_{ND} values.

The comparison of all previously published α7-nAChR radioligands (Table 1) revealed little correlation between $1/K_i$ and BP_{ND} (R^2 = 0.05, not shown). It was likely that the lack of correlation was due to the wide variability in binding assay conditions for these compounds when performed by various research groups (see Results and Discussion).

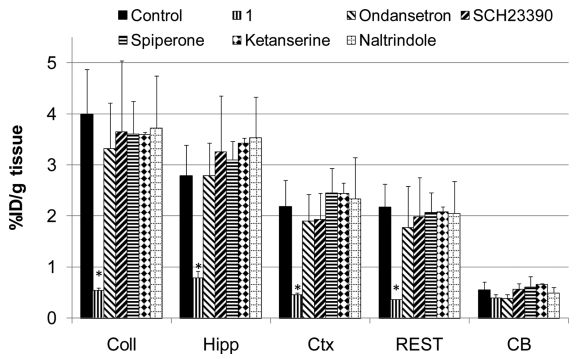

Figure 6. Effect of various CNS drugs (Table 5) on accumulation of [^{18}F]**7a** in CD-1 mouse brain regions 90 min after injection of tracer expressed as % ID/g tissue. Abbreviations: Coll, superior and inferior colliculus; Hipp, hippocampus; Ctx, cortex; CB, cerebellum; REST, rest of brain. Data are the mean ± SD (n = 3): (∗) P < 0.01, significantly different from controls. Columns that do not include the asterisk are insignificantly different from controls (P > 0.05) (ANOVA, single-factor analysis). The graph demonstrates that unlike the positive control (**1**) all non-α7-nAChR CNS drugs do not have an effect on the cerebral uptake of [^{18}F]**7a** and the radiotracer is α7-nAChR selective in vivo.

Table 5. CNS Drugs (2 mg/kg, sc) for α7-nAChR Selectivity Studies in Mice[a]

drug	target receptor	dose (mg/kg)	time of administration before radiotracer, min
1	selective α7-nAChR partial agonist	2	10
ondansetron	selective 5-HT$_3$ antagonist	2	10
SCH23390	D$_1$- and D$_5$-antagonist and 5-HT$_{1C/2C}$ agonist	2	10
spiperone	D$_2$-like and 5-HT$_{2A}$ receptor antagonist	2	10
ketanserin	5-HT$_2$/5-HT$_{2C}$ antagonist	2	10
naltrindole	selective δ-opioid antagonist	2	10

[a]5-HT = 5-hydroxytryptoamine (serotonin).

When the α7-nAChR binding assay for the radioligands is performed under the same assay conditions (Tables 2 and 3), the binding affinities $1/K_i$ correlate linearly (Figure 7) with the cortical BP_{ND} values of [^{18}F]**7a** and [^{18}F]**7c** (Table 4) and [^{11}C]**2**, [^{18}F]**3**, and [^{18}F]**4** (Table 1). This finding may explain why the specific binding of the very high affinity radioligands [^{18}F]**7a** and [^{18}F]**7c** is superior to the previous α7-nAChR radioligands with lower binding affinities. This result emphasizes further the importance of high binding affinity for the imaging properties of α7-nAChR radioligands.

CONCLUSION

A series of 3-(1,4-diazabicyclo[3.2.2]nonan-4-yl)dibenzo[*b*,*d*]-thiophene 5,5-dioxide derivatives with high binding affinities for α7-nAChRs (K_i = 0.4−20 nM) has been synthesized with potential application for PET imaging of α7-nAChRs. Two members of the series, **7a** and **7c**, with the best α7-nAChR

dx.doi.org/10.1021/jm401184f | J. Med. Chem. XXXX, XXX, XXX−XXX

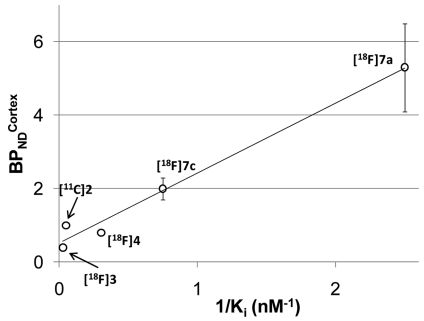

Figure 7. Correlation of the BP_{ND}^{cortex} (unitless) vs $1/K_i$ (nM^{-1}) of α7-nAChR PET radioligands [^{11}C]**2**, [^{18}F]**3**, [^{18}F]**4**, [^{18}F]**7a**, and [^{18}F]**7c** ($y = 1.91x + 0.52$; $R^2 = 0.98$). The BP_{ND} values are shown in Tables 1 and 3. The SD values are available for [^{18}F]**7a** and [^{18}F]**7c** only. All K_i values were obtained in this study under the same binding assay conditions (Tables 2 and 3).

binding affinities (K_i of 0.4 and 1.3 nM, respectively) and high selectivity vs other nicotinic subtypes and 5-HT_3, were radiolabeled with ^{18}F.

[^{18}F]**7a** and [^{18}F]**7c** readily entered the mouse brain and specifically and selectively labeled cerebral α7-nAChR receptors. The binding potential (BP_{ND}) values in mouse cortex of [^{18}F]**7a**, [^{18}F]**7c**, and previously published α7-nAChR radioligands correlated linearly with their binding affinities ($1/K_i$) when the binding affinity values were determined under the same assay conditions. In agreement with the binding affinity of [^{18}F]**7a** its BP_{ND} value in mice was substantially better than those of the previous α7-nAChR radioligands.

The best PET radioligand of this new series [^{18}F]**7a** exhibits excellent α7-nAChR imaging properties in the mouse brain. Therefore, [^{18}F]**7a** holds promise as a highly specific PET radioligand for quantification of α7-nAChR receptors, and further evaluation of this radioligand in baboon PET studies is underway.

EXPERIMENTAL SECTION

All reagents were used directly as obtained commercially unless otherwise noted. Reaction progress was monitored by TLC using silica gel 60 F254 (0.040−0.063 mm) with detection by UV. All moisture-sensitive reactions were performed under an argon atmosphere using oven-dried glassware and anhydrous solvents. Column flash chromatography was carried out using E. Merck silica gel 60F (230−400 mesh). Analytical thin-layer chromatography (TLC) was performed on aluminum sheets coated with silica gel 60 F_{254} (0.25 mm thickness, E. Merck, Darmstadt, Germany). Melting points were determined with a Fisher-Johns apparatus and were not corrected. ^{1}H NMR spectra were recorded with a Bruker-400 NMR spectrometer at nominal resonance frequencies of 400 MHz in $CDCl_3$ or DMSO-d_6 (referenced to internal Me_4Si at δ_H 0 ppm). The chemical shifts (δ) were expressed in parts per million (ppm). First order J values were given in hertz. Splitting patterns are described as singlet (s), doublet (d), triplet (t), quartet (q), and broad (br). High resolution mass spectra were recorded utilizing electrospray ionization (ESI) at the University of Notre Dame Mass Spectrometry facility. All compounds that were tested in the biological assays were analyzed by combustion analysis (CHN) to confirm the purity of >95%. Elemental analyses were determined by Galbraith Laboratories, Inc. (Knoxville, TN). The HPLC system consisted of two Waters model 600 pumps, two Rheodyne model 7126 injectors, an in-line Waters model 441 UV detector (254 nm), and a single sodium iodide crystal flow radioactivity detector. All HPLC chromatograms were recorded with Varian Galaxy software (version 1.8). The analytical and semi-preparative chromatographies were performed using Waters XBridge C-18 10 μm columns (analytical 4.6 mm × 250 mm and preparative 10 mm × 250 mm).

A dose calibrator (Capintec 15R) was used for all radioactivity measurements. Radiofluorination was performed with a modified GE MicroLab radiochemistry box.

Chemistry. Typical Procedure for Reduction of Nitro Derivatives to Anilines 12, 13, 19, 26, 27. A mixture of nitro compound (1 mmol), iron powder (4 mmol), ammonium chloride (1.2 mmol) in methanol (6 mL), THF (6 mL), and water (2 mL) was heated to reflux (80 °C) for 3 h. The resulting mixture was diluted with ethanol and concentrated and dried under vacuum. The residue was purified by silica gel column chromatography ($CHCl_3$/*i*-PrOH/Et_3N 10:1:0.1 to 10:30:4) to give the corresponding aniline derivative.

Typical Procedure for Bromination. *N*-Bromosuccinimide (NBS) (1 mmol) was added to a solution of the starting 1,4-dibenzothiophene derivative (1 mmol) in concentrated H_2SO_4 (3.6 mL) at room temperature. After 24 h, the solution was carefully poured into ice/water. The solids were filtered and washed with water and methanol. The obtained solids were recrystallized from 95% EtOH to afford the bromo compounds.

Typical Procedure for Oxidation of 1,4-Dibenzothiophene Derivatives. 1,4-Dibenzothiophene derivative (1 mmol) was dissolved in glacial acetic acid (2.8 mL) at room temperature. Aqueous hydrogen peroxide (30%, 1.4 mL) was added in small portions to the stirred solution. The addition of H_2O_2 resulted initially in some precipitation. The mixture was stirred at 60 °C for 24 h, then cooled to room temperature. The solid was filtered off, sequentially washed with 70% aqueous acetic acid, then 30% aqueous acetic acid, then water, and dried to afford the title compound.

3-Bromo-6-fluorodibenzo[*b*,*d*]thiophene 5,5-Dioxide (6a). The typical procedure for oxidation of 1,4-dibenzothiophene was followed, starting with **20** (600 mg, 2.13 mmol). The title compound **6a** (648 mg, 97%) was obtained as white crystals. ^{1}H NMR ($CDCl_3$, 400 MHz) δ 7.97 (s, 1H), 7.81 (dd, J = 12.0, 1.8 Hz, 1H), 7.68 (d, J = 8.0 Hz, 1H), 7.66 (dd, J = 8.0, 4.0 Hz, 1H), 7.59 (d, J = 8.0 Hz, 1H), 7.24 (t, J = 8.0 Hz, 1H).

3-Bromo-7-fluorodibenzo[*b*,*d*]thiophene 5,5-Dioxide (6b). A mixture of **26** (620 mg, 2 mmol) and 48% tetrafluoroboric acid (HBF_4) (4 mL) was stirred at 0−5 °C for 10 min. A cold solution of sodium nitrite (204 mg in 0.8 mL of water, 3 mmol) was added dropwise with stirring. After the mixture was stirred for 1 h at 0−5 °C the precipitated intermediate diazonium tetrafluoroborate was collected by filtration, washed with cold tetrafluoroboric acid (5%) and water and Et_2O, and dried under vacuum. The diazonium tetrafluoroborate was boiled in xylene (135 °C) for 120 min. The solvent was evaporated under reduced pressure. The residue was extracted with a mixture of chloroform and water. The chloroform layer was separated and concentrated. The residue was chromatographed on silica gel using hexanes−EtOAc (4:1) as eluent to give **6b** as a pale yellow solid (330 mg, 53%). ^{1}H NMR ($CDCl_3$, 400 MHz) δ 7.96 (d, J = 2.0 Hz, 1H), 7.81−7.77 (m, 2H), 7.64 (d, J = 8.0 Hz, 1H), 7.54 (dd, J = 8.0, 4.0 Hz, 1H), 7.40−7.35 (m, 1H)

7-Bromo-2-fluorodibenzo[*b*,*d*]thiophene 5,5-Dioxide (6c). A mixture of **27** (310 mg, 1 mmol) and 48% tetrafluoroboric acid (HBF_4) (2 mL) was stirred at 0−5 °C for 10 min. A cold solution of sodium nitrite (102 mg, 1.5 mmol) in 0.4 mL of water was added dropwise with stirring. After the mixture was stirred for 1 h at 0 −5 °C, the precipitated diazonium tetrafluoroborate was collected by filtration, washed with cold tetrafluoroboric acid (5%) and water and Et_2O, and dried under vacuum. The diazonium tetrafluoroborate was boiled in xylene (135 °C) for 30 min. The solvent was evaporated under reduced pressure. The residue was treated with chloroform and water. The chloroform layer was separated and concentrated. The residue was chromatographed on silica gel using hexanes−EtOAc (4:1) as eluent to give **6c** as a pale yellow solid (156 mg, 50%). ^{1}H NMR (DMSO-d_6, 400 MHz) δ 8.38 (d, J = 4.0 Hz, 1H), 8.23−8.18 (m, 2H), 8.13−8.07 (m, 2H), 7.54 (t, J = 8.0 Hz, 1H).

3-Bromo-4-fluorodibenzo[*b*,*d*]thiophene 5,5-Dioxide (6d) and 1-Bromo-4-fluorodibenzo[*b*,*d*]thiophene 5,5-Dioxide (6e). The typical procedure for bromination was followed, starting

dx.doi.org/10.1021/jm401184f | J. Med. Chem. XXXX, XXX, XXX−XXX

with **29** (905 mg, 3.86 mmol). Separation of the crude reaction product by silica gel chromatography using hexanes/ethyl acetate (5:2) yielded two isomers **6d** (285 mg, 0.91 mmol, 23.6%) and **6e** (160 mg, 0.51 mmol, 13%). The isomer **6e** was in the first chromatography fraction, whereas **6d** was in the second fraction.

6d: R_f = 0.31 (hexanes/EtOAc 2:1); ^{1}H NMR ($CDCl_3$, 400 MHz) δ 7.86−7.80 (m, 3H), 7.70 (t, J = 8.0 Hz, 1H), 7.63 (d, J = 8.0 Hz, 1H), 7.49 (d, J = 8.0 Hz, 1H).

6e: R_f = 0.5 (hexanes/EtOAc 2:1); ^{1}H NMR ($CDCl_3$, 400 MHz) δ 8.94 (d, J = 8.0 Hz, 1H), 7.90 (d, J = 8.0 Hz, 1H), 7.83−7.79 (m, 1H), 7.75 (dd, J = 8.0, 4.0 Hz, 1H), 7.67 (d, J = 8.0 Hz, 1H), 7.11 (t, J = 8.0 Hz, 1H).

Typical Procedure for Buchwald−Hartwig Cross-Coupling Reaction. 3-(1,4-Diazabicyclo[3.2.2]nonan-4-yl)-6-fluorodibenzo[*b*,*d*]thiophene 5,5-Dioxide (7a). A catalyst solution was prepared by mixing tris(dibenzylideneacetone)dipalladium ($Pd_2(dba)_3$, 58 mg, 0.063 mmol; Aldrich) and racemic BINAP (39 mg, 0.125 mmol; Strem) in toluene (4 mL) and heating the mixture to 90 °C for 15 min. The solution was cooled and then added to a mixture of 1,4-diazabicyclo[3.2.2]nonane (200 mg, 1.58 mmol) and **6a** (0.492 g, 1.58 mmol), in toluene (12 mL). Cs_2CO_3 (766 mg, 2.4 mmol; Aldrich) was then added, and the reaction mixture was flushed with nitrogen and heated overnight at 80−85 °C. After cooling to room temperature, the mixture was concentrated and purified by silica gel flash chromatography ($CHCl_3$/*i*-PrOH/Et_3N 10:1:0.2). The title compound **7a** (227 mg, 40% yield) was obtained as a yellow solid. ^{1}H NMR (DMSO-d_6, 400 MHz) δ 7.89 (d, J = 8.0 Hz, 1H), 7.77 (d, J = 8.0 Hz, 1H), 7.73 (t, J = 8.0 Hz, 1H), 7.29−7.24 (m, 2H), 7.12 (d, J = 8.0 Hz, 1H), 4.19 (s, 1H), 3.70−3.67 (m, 2H), 2.98−2.91 (m, 4H), 2.88−2.82 (m, 2H), 1.99 (m, 2H), 1.72−1.66 (m, 2H); HRMS calculated for $C_{19}H_{20}FN_2O_2S$ ([M + H]) 359.1224; found, 359.1240.

Preparation of 7a·*p*-TSA Salt. A mixture of **7a** (30 mg, 0.084 mmol) and *p*-toluenesulfonic acid monohydrate (19 mg, 0.099 mmol) was stirred in EtOAc−EtOH (2 mL, 10:1) at room temperature for 2 h. The resulting solid was collected, washed with EtOAc−EtOH (2 mL, 10:1) and EtOAc (3 mL), and dried under vacuum to afford the title compound as a yellow solid (32 mg, 72% yield). ^{1}H NMR (DMSO-d_6, 400 MHz) δ 10.10 (s, 1H), 7.99 (d, J = 8.0 Hz, 1H), 7.85 (d, J = 8.0 Hz, 1H), 7.79−7.73 (m, 1H), 7.49−7.45 (m, 3H), 7.32 (t, J = 8.0 Hz, 1H), 7.25 (dd, J = 8.0, 4.0 Hz, 1H), 7.12 (br s, 1H), 7.10 (br s, 1H), 4.47 (s, 1H), 3.95−3.93 (m, 2H), 3.49−3.39 (m, 6H), 2.29 (s, 3H), 2.19 (m, 2H), 2.05 (m, 2H). Elemental analysis for $C_{26}H_{27}FN_2O_5S_2$, calcd: C, 58.85; H, 5.13; N, 5.28. Found: C, 58.57; H, 5.04; N, 5.18.

4-(7-Fluorodibenzo[*b*,*d*]thiophen-3-yl)-1,4-diazabicyclo-[3.2.2]nonane 5,5-Dioxide (7b). The typical procedure for Buchwald−Hartwig cross-coupling reaction was followed, starting with **6b** (0.2 g, 0.64 mmol). The title compound **7b** was obtained as a yellow solid (104 mg, 0.29 mmol, 45% yield). ^{1}H NMR (DMSO-d_6, 400 MHz) δ 7.99 (dd, J = 8.0, 4.0 Hz, 1H), 7.89 (dd, J = 8.0, 3.0 Hz, 1H), 7.86 (d, J = 8.0 Hz, 1H), 7.55 (m, 1H), 7.25 (d, J = 4.0 Hz, 1H), 7.11 (dd, J = 8.0, 4.0 Hz, 1H), 4.17 (s, 1H), 3.66 (m, 2H), 2.99−2.91 (m, 3H), 2.87−2.82 (m, 3H), 2.00−1.97 (m, 2H), 1.71−1.65 (m, 2H). Elemental analysis for $C_{19}H_{19}FN_2O_2S{\cdot}0.1H_2O$, calcd: C, 62.37; H, 5.17; N, 7.58. Found: C, 62.25; H, 5.44; N, 7.19.

7-(1,4-Diazabicyclo[3.2.2]nonan-4-yl)-2-fluorodibenzo[*b*,*d*]-thiophene 5,5-Dioxide (7c). The typical procedure for Buchwald−Hartwig cross-coupling reaction was followed, starting with **6c** (0.226 g, 0.72 mmol), and the title compound **7c** (140 mg, 54% yield) was obtained as a yellow solid. ^{1}H NMR (DMSO-d_6, 400 MHz) δ 7.93−7.87 (m, 3H), 7.26−7.21 (m, 2H), 7.12 (d, J = 8.0 Hz, 1H), 4.20 (s, 1H), 3.71−3.68 (m, 2H), 3.01−2.83 (m, 6H), 2.00 (br s, 2H), 1.73−1.67 (m, 2H); HRMS calculated for $C_{19}H_{20}FN_2O_2S$ ([M + H]) 359.1224; found, 359.1241.

TSA salt: ^{1}H NMR (DMSO-d_6, 400 MHz) δ 10.08 (s, 1H), 8.00−7.94 (m, 3H), 7.48 (d, J = 8.0 Hz, 1H), 7.43 (m, 2H), 7.32−7.25 (m, 2H), 7.12 (br, 1H), 7.10 (br, 1H), 4.48 (s, 1H), 3.94 (m, 2H), 3.47−3.38 (m, 6H), 2.29 (s, 3H), 2.19 (m, 2H), 2.06−1.99 (m, 2H). Elemental analysis for $C_{26}H_{27}FN_2O_5S_2{\cdot}0.75H_2O$, calcd: C, 57.39; H, 5.28; N, 5.15. Found: C, 57.22; H, 5.11; N, 5.12.

3-(1,4-Diazabicyclo[3.2.2]nonan-4-yl)-4-fluorodibenzo[*b*,*d*]-thiophene 5,5-Dioxide (7d). The typical procedure for Buchwald−Hartwig cross-coupling reaction was followed, starting with **6d** (0.246 g, 0.78 mmol), and the title compound **7d** was obtained as a yellow solid (170 mg, 0.47 mmol, 60% yield). Free base: ^{1}H NMR (DMSO-d_6, 400 MHz) δ 8.06 (d, J = 8.0 Hz, 1H), 7.91 (d, J = 8.0 Hz, 1H), 7.81 (d, J = 8.0 Hz, 1H), 7.75 (t, J = 8.0 Hz, 1H), 7.54 (t, J = 8.0 Hz, 1H), 7.36 (t, J = 8.0 Hz, 1H), 3.82 (s, 1H), 3.43−3.40 (m, 2H), 3.03−3.00 (m, 2H), 2.93−2.89 (m, 4H), 2.00−1.97 (m, 2H), 1.74−1.66 (m, 2H); HRMS calculated for $C_{19}H_{20}FN_2O_2S$ ([M + H]) 359.1224; found, 359.1246.

TSA salt: ^{1}H NMR (DMSO-d_6, 400 MHz) δ 10.16 (s, 1H), 8.12 (br s, 1H), 7.94−7.90 (m, 2H), 7.78 (d, J = 8.0 Hz, 1H), 7.59 (d, J = 8.0 Hz, 1H), 7.50−7.40 (m, 3H), 7.12 (m, 2H), 4.01 (s, 1H), 3.54−3.38 (m, 6H), 2.30 (s, 3H), 2.19 (s, 2H), 2.07 (s, 2H), 1.09−1.03 (m, 2H). Elemental analysis for $C_{26}H_{27}FN_2O_5S_2{\cdot}0.5H_2O$, calcd: C, 57.87; H, 5.23; N, 5.19. Found: C, 58.21; H, 5.56; N, 4.88.

1-(1,4-Diazabicyclo[3.2.2]nonan-4-yl)-4-fluorodibenzo[*b*,*d*]-thiophene 5,5-Dioxide (7e). The typical procedure for Buchwald−Hartwig cross-coupling reaction was followed, starting with **6e** (0.112 g, 0.36 mmol). The title compound **7e** was obtained as a yellow solid (52 mg, 0.15 mmol, 40% yield). ^{1}H NMR ($CDCl_3$, 400 MHz) δ 8.50 (d, J = 8.0 Hz, 1H), 7.84 (d, J = 8.0 Hz, 1H), 7.68 (t, J = 8.0 Hz, 1H), 7.55 (t, J = 8.0 Hz, 1H), 7.43 (dd, J = 8.0, 4.0 Hz, 1H), 7.14 (t, J = 8.0 Hz, 1H), 3.66−3.63 (m, 1H), 3.29−3.21 (m, 5H), 3.14−3.09 (m, 2H), 2.16−2.10 (m, 2H), 1.87−1.71 (m, 3H); HRMS calculated for $C_{19}H_{20}FN_2O_2S$ ([M + H]) 359.1224; found, 359.1215. Elemental analysis for $C_{19}H_{19}FN_2O_2S{\cdot}1.5H_2O$, calcd: C, 59.20; H, 5.75; N, 7.27. Found: C, 58.90; H, 5.76; N, 7.10.

3-Bromo-6-nitrodibenzo[*b*,*d*]thiophene 5,5-Dioxide (8). The typical procedure for bromination was followed, starting with **31** (1.96 g, 7.5 mmol), and compound **8** was obtained as a pale brown solid (1.73 g, 77%). ^{1}H NMR (DMSO-d_6, 400 MHz) δ 8.70 (d, J = 8.0 Hz, 1H), 8.45−8.43 (m, 2H), 8.28 (d, J = 8.0 Hz, 1H), 8.14−8.09 (m, 2H). HRMS calculated for $C_{12}H_6BrNNaO_4S$ ($[M + Na]^+$) 361.9093; found, 361.9080.

7-Bromo-2-nitrodibenzo[*b*,*d*]thiophene 5,5-Dioxide (9). The typical procedure for bromination was followed, starting with **24** (1.82 g, 6.95 mmol), and compound **9** (2.1 g, 89%) was obtained as a pale yellow solid. ^{1}H NMR (DMSO-d_6, 400 MHz) δ 9.10 (s, 1H), 8.44−8.47 (m, 3H), 8.33 (d, J = 8.0 Hz, 1H), 8.11 (dd, J = 8.0, 4.0 Hz, 1H).

3-(1,4-Diazabicyclo[3.2.2]nonan-4-yl)-6-nitrodibenzo[*b*,*d*]-thiophene 5,5-Dioxide (10). The typical procedure for Buchwald−Hartwig cross-coupling reaction was followed starting with **8** (0.129 g, 0.38 mmol). Note that the reaction mixture was heated at 105 °C for 48 h. The title compound **10** was obtained as a reddish solid (80 mg, 55% yield). ^{1}H NMR (DMSO-d_6, 400 MHz) δ 8.40 (d, J = 4.0 Hz, 1H), 8.15 (d, J = 8.0 Hz, 1H), 7.97 (d, J = 8.0 Hz, 1H), 7.94 (d, J = 8.0 Hz, 1H), 7.26 (d, J = 4.0 Hz, 1H), 7.15 (d, J = 4.0 Hz, 1H), 4.21 (s, 1H), 3.71 (m, 2H), 3.00−2.85 (m, 6H), 2.00 (s, 2H), 1.71 (m, 2H); HRMS calculated for $C_{19}H_{20}N_3O_4S$ ([M + H]) 386.1169; found, 386.1150. Elemental analysis for $C_{19}H_{19}N_3O_4S{\cdot}H_2O$, calcd: C, 56.56; H, 5.25; N, 10.42. Found: C, 56.65; H, 4.99; N, 10.50.

7-(1, 4-Diazabicyclo[3.2.2]nonan-4-yl)-2-nitrodibenzo[*b*,*d*]-thiophene 5,5-Dioxide (11). The typical procedure for Buchwald−Hartwig cross-coupling reaction was followed, starting with **9** (1.83 g, 5.38 mmol). The title compound **11** was obtained as a reddish solid (0.836 g, 61% yield). ^{1}H NMR (DMSO-d_6, 400 MHz) δ 8.77 (s, 1H), 8.20−8.12 (m, 3H), 7.32 (d, J = 4.0 Hz, 1H), 7.16 (dd, J = 8.0, 4.0 Hz, 1H), 4.23 (s, 1H), 3.72 (m, 2H), 3.00−2.88 (m, 6H), 2.00 (br s, 2H), 1.74−1.69 (m, 2H); HRMS calculated for $C_{19}H_{20}N_3O_4S$ ([M + H]) 386.1169; found, 386.1152. Elemental analysis for $C_{19}H_{19}N_3O_4S{\cdot}1.25H_2O$, calcd: C, 55.94; H, 5.31; N, 10.30. Found: C, 55.98; H, 5.17; N, 10.15.

6-Amino-3-(1,4-diazabicyclo[3.2.2]nonan-4-yl)-dibenzo[*b*,*d*]-thiophene 5,5-Dioxide (12). The typical procedure for reduction of nitro derivatives was followed starting with **10** (0.34 g, 0.88 mmol), and compound **12** (146 mg, 46%) was obtained as a yellow solid. ^{1}H NMR (DMSO-d_6, 400 MHz) δ 7.73 (d, J = 12.0 Hz, 1H), 7.25 (t, J = 8.0 Hz, 1H), 7.11 (br s, 1H), 7.05 (d, J = 8.0 Hz, 1H), 6.97 (d, J = 4.0

dx.doi.org/10.1021/jm401184f | J. Med. Chem. XXXX, XXX, XXX−XXX

Hz, 1H), 6.62 (d, J = 8.0 Hz, 1H), 5.87 (br s, 2 H), 4.17 (s, 1H), 3.66 (m, 2H), 2.98−2.91 (m, 6H), 2.01 (s, 2H), 1.72 (m, 2H).

2-Amino-7-(1,4-diazabicyclo[3.2.2]nonan-4-yl)dibenzo[*b*,*d*]-thiophene 5,5-Dioxide (13). The typical procedure for reduction of nitro derivatives was followed starting with **11** (0.68 g, 1.76 mmol), and compound **13** was obtained as a yellow solid (585 mg, 93%). ^{1}H NMR (DMSO-d_6, 400 MHz) δ 7.67 (d, J = 12 Hz, 1H), 7.43 (d, J = 12 Hz, 1H), 7.27 (s, 1H), 7.14 (d, J = 8.0, 4.0 Hz, 1H), 6.91 (s, 1H), 6.53 (d, J = 8.0, 4.0 Hz, 1H), 6.17 (s, 2H), 4.40 (s, 1H), 3.87 (br s, 3H), 3.07 (m, 1H), 2.15 (br s, 3H), 2.02 (br s, 3H), 1.20 (m, 2H).

3-(1,4-Diazabicyclo[3.2.2]nonan-4-yl)-6-iododibenzo[*b*,*d*]-thiophene 5,5-Dioxide (14). Compound **12** (143 mg, 0.4 mmol) was dissolved in a mixture of 4 N H_2SO_4 (0.8 mL) and CH_3CN (1 mL), and the solution was cooled to −5 °C. Sodium nitrite (55 mg, 0.8 mmol) dissolved in H_2O (0.5 mL) was added dropwise at the same temperature. After the mixture was stirred for 60 min a solution of diazonium salt was formed. To a mixture of CuI (268 mg, 1.4 mmol) and saturated KI solution (2.5 mL) at 70 °C was added the above-prepared solution of diazonium salt dropwise over 10 min, and the mixture was further stirred at 70 °C for 30 min. The reaction mixture was cooled, and 28% ammonia solution was added (2 mL). The aqueous suspension was repeatedly extracted with $CHCl_3$ and the combined organic layers were washed with brine (10 mL), dried (Na_2SO_4), and concentrated in vacuo. The crude product was purified by flash chromatography on silica gel ($CHCl_3$/*i*-PrOH/Et_3N 10:1:0.1 to 3:1:0.2) to give **14** (28 mg, 15%). ^{1}H NMR (DMSO-d_6, 400 MHz) δ 7.96 (d, J = 8.0 Hz, 1H), 7.92 (d, J = 4.0 Hz, 1H), 7.81 (d, J = 8.0 Hz, 1H), 7.38 (t, J = 8.0 Hz, 1H), 7.32 (d, J = 4.0 Hz, 1H), 7.18 (d, J = 8.0 Hz, 1H), 4.34 (s, 1H), 3.82 (m, 2H), 3.22−3.18 (m, 6H), 2.09 (m, 2H), 1.87 (m, 2H). Elemental analysis for $C_{19}H_{19}IN_2O_2S{\cdot}2.5H_2O$, calcd: C, 44.63; H, 4.73; N, 5.48. Found: C, 44.88; H, 4.41; N, 5.48.

7-(1,4-Diazabicyclo[3.2.2]nonan-4-yl)-2-iododibenzo[*b*,*d*]-thiophene 5,5-Dioxide (15). Compound **13** (285 mg, 0.8 mmol) was dissolved in a mixture of 4 N H_2SO_4 (1.5 mL) and CH_3CN (2 mL), and the solution was cooled to −5 °C. $NaNO_2$ (110 mg, 1.6 mmol, 2 equiv) dissolved in H_2O (1 mL) was added dropwise at the same temperature. After the mixture was stirred for 60 min a solution of diazonium salt was formed. To a mixture of CuI (536 mg, 2.8 mmol, 3.5 equiv) and saturated KI solution (2.5 mL) at 70 °C was added above-prepared solution of diazonium salt dropwise over 10 min and further stirred at 70 °C for 30 min. The reaction mixture was cooled, and saturated NH_4OH was added (4 mL). The aqueous suspension was repeatedly extracted with $CHCl_3$, and the combined organic layers were washed with brine (10 mL), dried (Na_2SO_4), and concentrated in vacuo. The crude product was purified by flash chromatography on silica gel ($CHCl_3$/*i*-PrOH/Et_3N 10:1:0.1 to 3:1:0.2) to give **15** (75 mg, 20%). ^{1}H NMR (DMSO-d_6, 400 MHz) δ 8.40 (d, J = 4.0 Hz, 1H), 7.93 (d, J = 8.0 Hz, 1H), 7.78 (dd, J = 8.0, 1.8 Hz, 1H), 7.60 (d, J = 12.0 Hz, 1H), 7.25 (d, J = 1.8 Hz, 1H), 7.11 (dd, J = 8.0, 4.0 Hz, 1H), 4.20 (s, 1H), 3.70 (m, 2H), 2.98−2.88 (m, 6H), 2.00 (s, 2H), 1.72 (m, 2H); HRMS calculated for $C_{19}H_{20}IN_2O_2S$ ([M + H]) 467.0285; found, 467.0306;. Elemental analysis for $C_{19}H_{21}IN_2O_3S$, calcd: C, 47.12; H, 4.37; N, 5.78. Found: C, 47.24; H, 4.53; N, 5.87.

(5-Bromo-2-nitrophenyl)(2-fluorophenyl)sulfane (18). Cesium carbonate (4.3 g, 13.2 mmol) was added to a solution of 4-bromo-2-fluoronitrobenzene **16** (2.42, 11 mmol, Aldrich) and 2-fluorobenzene thiol **17** (1.4 g, 11 mmol, Aldrich) in DMF (60 mL), and the mixture was stirred for 5 h at room temperature. Water (200 mL) and ethyl acetate (100 mL) were added. The organic layer was separated and washed sequentially with water (100 mL) and then brine (100 mL). The organic phase was separated, dried, and concentrated to yield a yellow solid that was purified by silica gel chromatography (hexanes/EtOAc 8:1 to 3:1) to give **18** (2.88 g, 80%). ^{1}H NMR ($CDCl_3$, 400 MHz) δ 8.17 (d, J = 8.0 Hz, 1H), 7.68−7.60 (m, 2H), 7.41−7.29 (m, 3H), 6.95 (s, 1H).

4-Bromo-2-((2-fluorophenyl)thio)aniline (19). The typical procedure for reduction of nitro derivatives was followed, starting with **18** (3.2 g, 9.75 mmol), and the title compound **19** was obtained as a brown solid (2.46 g, 85%). ^{1}H NMR ($CDCl_3$, 400 MHz) δ 7.59 (d, J = 4.0 Hz, 1H), 7.33 (dd, J = 8.0, 4.0 Hz, 1H), 7.21−7.15 (m, 1 H), 7.10−7.00 (m, 2H), 6.92−6.87 (m, 1H), 6.69 (d, J = 8.0 Hz, 1H), 4.37 (br s, 2H).

3-Bromo-6-fluorodibenzo[*b*,*d*]thiophene (20). Compound **19** (1.18 g, 3.96 mmol) was dissolved in 37% HCl (11 mL), and the solution was cooled below 5 °C. To this reaction mixture, sodium nitrite (408 mg, 5.93 mmol) was added slowly at a temperature below 5 °C. After addition, the mixture was stirred for 30 min below 5 °C. Then sodium tetrafluoroborate (865 mg, 7.92 mmol) was added, and the reaction mixture was stirred for another 30 min at a temperature below 5 °C. This reaction solution was then added to the stirred solution of copper(I) oxide (1.14 mg, 7.92 mmol) in 0.1 N sulfuric acid (390 mL) at 35−40 °C. The reaction mixture was stirred for 15−30 min. Ethyl acetate was added to the reaction mixture, and the mixture was filtered to remove inorganic compound. The filtrate was then extracted with ethyl acetate (3 × 120 mL). The organic extract was washed with water followed by brine and then concentrated under vacuum. The residue was purified by silica gel chromatography (hexanes) to give **20** (600 mg, 54%). ^{1}H NMR ($CDCl_3$, 400 MHz) δ 8.04 (d, J = 4.0 Hz, 1H), 8.02 (d, J = 8.0 Hz, 1H), 7.93 (d, J = 8.0 Hz, 1H), 7.62 (dd, J = 8.0, 4.0 Hz, 1H), 7.47 (ddd, J = 12.0, 8.0, 4.0 Hz, 1H), 7.22 (t, J = 8.0 Hz, 1H).

3-Nitrodibenzo[*b*,*d*]thiophene 5,5-Dioxide (23). Dibenzo-[*b*,*d*]thiophene 5,5-dioxide **21** (10 g, 46 mmol, Aldrich) was slowly added to a stirred mixture of glacial acetic acid (34 mL) and sulfuric acid (96%, 34 mL). The slurry was stirred, and red fuming nitric acid (36 mL) was added dropwise over a period of 90 min at temperature −5 °C to 5 °C. The slurry was stirred for another 30 min and poured over ice. The precipitate was filtered, rinsed with water, and dried at room temperature. The crude product was recrystallized with acetonitrile to give **23** as yellow crystals (8.7 g, 72%). ^{1}H NMR (DMSO-d_6, 400 MHz) δ 8.84 (d, J = 8.0 Hz, 1H), 8.65 (dd, J = 8.0, 2.0 Hz, 1H), 8.50 (d, J = 8.0 Hz, 1H), 8.39 (d, J = 8.0 Hz, 1H), 8.13 (d, J = 8.0 Hz, 1H), 7.93 (t, J = 8.0 Hz, 1H), 7.81 (t, J = 8.0 Hz, 1H).

2-Nitrodibenzo[*b*,*d*]thiophene 5,5-Dioxide (24). The typical procedure for oxidation of 1,4-dibenzothiophene was followed starting with **22** (489 mg, 2.13 mmol, Oakwood Chemical), and the title compound **24** (510 mg, 90%) was obtained as white crystals. ^{1}H NMR ($CDCl_3$, 400 MHz) δ 8.66 (d, J = 4 Hz, 1H), 8.43 (dd, J = 8, 4 Hz, 1H), 8.04 (d, J = 8 Hz, 1H), 7.96 (d, J = 8 Hz, 1H), 7.92 (d, J = 8 Hz, 1H), 7.79 (t, J = 8 Hz, 1H), 7.69 (t, J = 8.0 Hz, 1H).

3-Bromo-7-nitrodibenzo[*b*,*d*]thiophene 5,5-Dioxide (25). The typical procedure for bromination was followed starting with **23** (2.59 g, 9.9 mmol), and brown solid was obtained and recrystallized with benzene to yield **25** as a yellow solid (1.73 g, 51%). ^{1}H NMR (DMSO-d_6, 400 MHz) δ 8.89 (d, J = 4.0 Hz, 1H), 8.67 (dd, J = 8.0, 3.0 Hz, 1H), 8.52−8.49 (m, 2H), 8.35 (d, J = 8.0 Hz, 1H), 8.15 (dd, J = 8.0, 2.0 Hz, 1H).

7-Bromodibenzo[*b*,*d*]thiophen-3-amine 5,5-Dioxide (26). A solution of stannous chloride dihydrate (12.4 g, 56 mmol) in 37% hydrochloric acid (21 mL) was added to a mixture of **25** (1.7 g, 5 mmol) in glacial acetic acid (50 mL). The reaction mixture was stirred at 100 °C for 60 min and cooled to 5 °C. The precipitate was filtered off, rinsed with water on the filter, and dispersed in water. The dispersion was made basic (pH 10) by addition of an excess of 1 M sodium hydroxide and stirred for 3 h. The precipitate was filtered off, rinsed with water, and dried overnight on the filter to yield **26** (0.7 g, 45%) as a pale white solid. ^{1}H NMR (DMSO-d_6, 400 MHz) δ 8.12 (s, 1H), 7.87−7.77 (m, 3H), 6.95 (s, 1H), 6.87 (dd, J = 8, 4 Hz, 1H), 6.20 (br s, 2H).

2-Amino-7-bromodibenzo[*b*,*d*]thiophene 5,5-Dioxide (27). The typical procedure for reduction of nitro derivatives was followed starting with **9** (0.60 g, 1.76 mmol). The title compound **27** (496 mg, 91%) was obtained as a white solid. ^{1}H NMR (DMSO-d_6, 400 MHz) δ 8.16 (d, J = 4 Hz, 1H), 7.93(d, J = 8.0 Hz, 1H), 7.87 (d, J = 12 Hz, 1H), 7.56 (d, J = 8 Hz, 1H), 7.08 (s, 1H), 6.71 (d, J = 8 Hz, 1H), 6.36 (br s, 2H).

4-Fluorodibenzo[*b*,*d*]thiophene 5,5-Dioxide (29). The typical procedure for oxidation of 1,4-dibenzothiophene was followed starting with 4-fluorodibenzo[*b*,*d*]thiophene **28**[45] (1.62 g, 8 mmol). The title compound **29** (1.8 g, 96%) was obtained as white crystals. ^{1}H NMR

dx.doi.org/10.1021/jm401184f | J. Med. Chem. XXXX, XXX, XXX−XXX

Table 6. HPLC Conditions for [^{18}F]7a and [^{18}F]7c

	column	mobile phase	flow rate, mL/min	product retention time, min	nitro precursor retention time, min
[^{18}F]**7a**, preparative	XBridge C18 column, 10 μm (250 mm × 10 mm)	$CH_3OH/CH_3CN/H_2O/Me_3N$ 260:120:620:2	12	32	21
[^{18}F]**7a**, analytical	XBridge C18 column, 5 μm (250 mm × 4.6 mm)	$CH_3CN/H_2O/Et_3N$ 390:610:1	2	7.4	5.5
[^{18}F]**7c**, preparative	XBridge C18 column, 10 μm (150 mm × 10 mm)	$CH_3CN/H_2O/NH_3$ 280:720:1	10	20	27
[^{18}F]**7c**, analytical	XBridge C18 column, 3.5 μm (100 mm × 4.6 mm)	$CH_3CN/H_2O/NH_3$ 380:620:1	2	3.4	5.2

($CDCl_3$, 400 MHz) δ 7.85 (d, J = 8.0 Hz, 1H), 7.82 (d, J = 8.0 Hz, 1H), 7.71−7.57 (m, 4H), 7.20 (t, J = 8.0 Hz, 1H).

4-Nitrodibenzo[*b*,*d*]thiophene 5,5-Dioxide (31). The typical procedure for oxidation of 1,4-dibenzothiophene was followed starting with **30**[46] (1.08 g, 4.71 mmol). The final compound **31** (1.1g, 90%) was obtained as pale yellow crystals. ^{1}H NMR (DMSO-d_6, 400 MHz) δ 8.69 (d, J = 8.0 Hz, 1H), 8.42 (d, J = 8.0 Hz, 1H), 8.33 (d, J = 8.0 Hz, 1H), 8.11 (t, J = 8.0 Hz, 1H), 8.07 (d, J = 8.0 Hz, 1H), 7.88 (t, J = 8.0 Hz, 1H), 7.77 (t, J = 8.0 Hz, 1H). HRMS calculated for $C_{12}H_7NNaO_4S$ ([M + Na]) 283.9988; found, 283.9994.

Radiosynthesis of [^{18}F]7a and [^{18}F]7c. The same radiolabeling method was used for both radioligands [^{18}F]**7a** and [^{18}F]**7c**. A solution of the [^{18}F]fluoride, 15−20 mg of Kryptofix 222, and 1−2 mg of $K_2C_2O_4$ in 1 mL of 50% aqueous acetonitrile was added to a reaction vessel of a GE MicroLab box. The mixture was heated at 120−135 °C under a stream of argon, while water was evaporated azeotropically after the addition of 2 mL of CH_3CN. A solution of the corresponding nitro precursor (**10** or **11**) (2 mg) in anhydrous DMSO (0.8 mL) was added to the reaction vessel and heated at 160 °C for 12 min. The reaction mixture was cooled, diluted with 0.7 mL of water, and injected onto the reverse-phase semipreparative HPLC column (Table 6). The radioactive peak was collected in 50 mL of HPLC water. The water solution was transferred through an activated Waters C-18 Oasis HLB light solid-phase extraction (SPE) cartridge. After the SPE was washed with 10 mL of saline, the product was eluted with a mixture of 1 mL of ethanol and 0.04 mL of 1 N HCl through a 0.2 μm sterile filter into a sterile, pyrogen-free multidose vial and 10 mL of 0.9% saline and 0.05 mL of sterile 8.4% solution sodium bicarbonate were added through the same filter. The final products [^{18}F]**7a** and [^{18}F]**7c** were then analyzed by analytical HPLC (Table 6) using a UV detector at 340 nm to determine the radiochemical purity and specific radioactivity at the time synthesis ended. The total synthesis time including QC was 70−80 min.

In Vitro Binding Assay. α7-nAChR Assay with Rat Brain Membranes. The assay was done commercially by Caliper PerkinElmer (Hanover, MD). In brief, rat cortical membranes were incubated with [^{125}I]α-bungarotoxin (K_D = 0.7 nM) at 0.1 nM in a buffer consisting of 50 mM Tris, 120 mM NaCl, 5 mM KCl, 2 mM $CaCl_2$, 1 mM $MgCl_2$, 0.003 mM atropine sulfate at pH 7.4 for 150 min at 0 °C.[63] The binding was terminated by rapid vacuum filtration of the assay contents onto GF/C filters presoaked in PEI. Radioactivity trapped onto the filters was assessed using a γ-counter. Nonspecific binding was defined as that remaining in the presence of 1 μM α-bungarotoxin. The assays were done two times independently, each in duplicate, at multiple concentrations of the test compounds. Binding assay results were analyzed using a one-site competition model, and IC_{50} curves were generated based on a sigmoidal dose response with variable slope. The K_i values were calculated using the Cheng−Prusoff equation. Methyllycaconitine (MLA) was used as a reference compound in all assays.

HEK 293 Cell Culture and Stable Transfections (Heteromeric nAChR). HEK 293 cells (ATCC CRL 1573) were maintained at 37 °C with 5% CO_2 in a humidified incubator. Growth medium for the HEK 293 cells was the minimum essential medium supplemented with 10% fetal bovine serum, 100 units/mL penicillin G, and 100 μg/mL streptomycin. Transfections of these cells and selection and establishment of stable cell lines were carried out as described previously.[52,55]

Membrane Homogenate Preparation (Heteromeric nAChR). Membrane homogenates for ligand binding assays were made as described previously.[52,55] Briefly, cultured cells at >90% confluency were removed from the culture flask (80 cm^2) with a disposable cell scraper and placed in 10 mL of 50 mM Tris-HCl buffer (pH 7.4, 4 °C). The cell suspension was centrifuged at 1000g for 5 min, and the pellet was collected. The cell pellet was then homogenized in 10 mL of buffer with a Polytron homogenizer for 20 s and centrifuged at 35000g for 10 min at 4 °C. Membrane pellets were resuspended in fresh buffer.

Binding to Heteromeric nAChR. Binding to heteromeric nAChR subunit combinations, which represent possible heteromeric nAChRs, was measured with 0.5 nM [^{3}H]epibatidine in HEK cells expressing these subunits (K_D = 0.021 nM ($\alpha2\beta2$-nAChR), K_D = 0.084 nM ($\alpha2\beta4$-nAChR), K_D = 0.034 nM ($\alpha3\beta2$-nAChR), K_D = 0.29 nM ($\alpha3\beta4$-nAChR), K_D = 0.046 nM ($\alpha4\beta2$-nAChR), K_D = 0.094 nM ($\alpha4\beta4$-nAChR)).[55] Aliquots of the membrane homogenates containing 30−200 μg of protein were used for the binding assays, which were carried out in a final volume of 100 μL in borosilicate glass tubes. After incubation at 24 °C for 2 h, the samples were collected with a cell harvester (Brandel M-48) onto Whatman GF/C filters prewet with 0.5% polyethylenimine. After the samples were harvested, the filters were washed three times with 5 mL of 50 mM Tris-HCl buffer and then counted in a liquid scintillation counter. Nonspecific binding was measured in samples incubated in parallel containing 300 μM nicotine for [^{3}H]epibatidine binding. Specific binding was defined as the difference between total binding and nonspecific binding. Data from these competition binding assays were analyzed using Prism 5 (GraphPad Software, San Diego, CA).

5-HT$_3$(h) Binding Assay. The assay was done commercially by Caliper PerkinElmer (Hanover, MD) using recombinant HEK293 cells and 0.35 nM [^{3}H]GR65630 (K_D = 0.5 nM).

Biodistribution Studies in CD-1 Mice. Baseline Study. Male CD-1 mice weighing 25−30 g from Charles River Laboratories (Wilmington, MA) were used for biodistribution studies. The animals were sacrificed by cervical dislocation at various times following injection of [^{18}F]**7a** or [^{18}F]**7c** (70 μCi, specific radioactivity 8000−12000 mCi/μmol, in 0.2 mL of saline) into a lateral tail vein, three animals per time point. The brains were rapidly removed and dissected on ice. The brain regions of interest were weighed, and their radioactivity content was determined in an automated γ-counter with a counting error below 3%. Aliquots of the injectate were prepared as standards, and their radioactivity content was counted along with the tissue samples. The percent of injected dose per gram of tissue (%ID/g tissue) was calculated. All experimental protocols were approved by the Animal Care and Use Committee of the Johns Hopkins Medical Institutions.

Self-Blockade of [^{18}F]7a Binding with 7a. In vivo saturation blockade studies were done by iv coadministration of the radiotracer [^{18}F]**7a** (70 μCi, SA = 9200 mCi/μmol, 0.2 mL) with various doses of "cold" **7a** per animal (0 μg (vehicle), 0.0048 μg, 7.2 μg). Compound **7a** was dissolved in saline at pH 5.5. At 90 min after administration of the tracer and blocker, brain tissues were harvested, and their regional radioactivity content was determined. The self-blockade of [^{18}F]**7c** with **7c** was done similarly.

Blockade of [^{18}F]7a Binding with 1. In vivo α7-nAChR receptor blocking studies were done by intravenous coadministration of the

dx.doi.org/10.1021/jm401184f | J. Med. Chem. XXXX, XXX, XXX−XXX

radiotracer [^{18}F]**7a** (70 μCi, SA = 7900 mCi/μmol, 0.2 mL) with various doses of **1** (0 μg (vehicle), 0.02 mg/kg, 0.2 mg/kg, 1 mg/kg, and 3 mg/kg). Three animals per dose were used. **1** was dissolved in a vehicle (saline/alcohol (9:1) at pH 5.5). At 90 min after administration of the tracer, brain tissues were harvested, and their regional radioactivity content was determined. The dose-dependent blockade study of [^{18}F]**7c** with **5** was done the same way.

Blockade of [^{18}F]7a with Nicotine and Cytisine. In vivo CB1 receptor blocking studies were carried out by subcutaneous (sc) administration of (−)-nicotine tartrate (5 mg/kg) or cytisine (1 mg/kg) followed by iv injection of the radiotracer [^{18}F]**7a** (70 μCi, specific radioactivity of ∼14 000 mCi/μmol, 0.2 mL) 5 min thereafter. The drugs were dissolved in saline and administered in a volume of 0.1 mL. Control animals were injected with 0.1 mL of saline. At 90 min after administration of the tracer, brain tissues were harvested, and their radioactivity content was determined.

Blockade of [^{18}F]7a with Non-α7-nAChR Drugs. In vivo receptor blocking studies were performed by administration of six drugs (Table 5), followed by iv injection of the radiotracer [^{18}F]**7a** (70 μCi, specific radioactivity of ∼14 000 mCi/μmol, 0.2 mL). The drugs (2 mg/kg, sc) were dissolved in a vehicle (saline/DMSO 5:1) and administered in a volume of 0.1 mL. Control animals were injected with 0.1 mL of the vehicle solution. At 90 min after administration of the tracer, brain tissues were harvested, and their radioactivity content was determined.

AUTHOR INFORMATION

Corresponding Author

*Phone: 410-614-5130. Fax: 410-614-0111. E-mail: ahorti1@jhmi.edu.

Notes

The authors declare no competing financial interest.

ACKNOWLEDGMENTS

We thank Dr. Richard Wahl for fruitful discussions. We thank Dr. Hiroto Kuwabara for reading the manuscript and for his useful comments. We thank Dr. Yuchuan Wang for useful comments and references. We are grateful to Paige Finley and Gilbert Green for their valuable help with animal experiments. We are thankful to Judy W. Buchanan for editorial help. We very much thank Drs. Peter Brust (Helmholtz-Zentrum Dresden-Rossendorf Institute of Radiopharmacy) and Dan Peters (DanPET AB) for the samples of compounds **2** and **3** and Dr. Martin Pomper for the sample of **4** for our inhibition binding assay studies. This research was supported by NIH Grants MH079017 and AG037298 (A.G.H.) and in part by the Division of Nuclear Medicine of The Johns Hopkins University School of Medicine.

ABBREVIATIONS USED

BINAP, 2,2′-bis(diphenylphosphino)-1,1′-binaphthyl; B_{max}, receptor density in tissue; BP_{ND}, binding potential; EtOAc, ethyl acetate; EtOH, ethanol; Et_2O, diethyl ether; Et_3N, triethylamine; K_D, dissociation constant of the radioligand−receptor complex; nAChR, nicotinic acetylcholine receptor; *i*-PrOH, isopropyl alcohol

REFERENCES

(1) Gotti, C.; Clementi, F. Neuronal nicotinic receptors: from structure to pathology. *Prog. Neurobiol.* **2004**, *74*, 363−396.

(2) Lukas, R. J.; Changeux, J. P.; Le Novere, N.; Albuquerque, E. X.; Balfour, D. J.; Berg, D. K.; Bertrand, D.; Chiappinelli, V. A.; Clarke, P. B.; Collins, A. C.; Dani, J. A.; Grady, S. R.; Kellar, K. J.; Lindstrom, J. M.; Marks, M. J.; Quik, M.; Taylor, P. W.; Wonnacott, S. International Union of Pharmacology. XX. Current status of the nomenclature for nicotinic acetylcholine receptors and their subunits. *Pharmacol. Rev.* **1999**, *51*, 397−401.

(3) Dani, J. A.; Bertrand, D. Nicotinic acetylcholine receptors and nicotinic cholinergic mechanisms of the central nervous system. *Annu. Rev. Pharmacol. Toxicol.* **2007**, *47*, 699−729.

(4) Philip, N. S.; Carpenter, L. L.; Tyrka, A. R.; Price, L. H. Nicotinic acetylcholine receptors and depression: a review of the preclinical and clinical literature. *Psychopharmacology (Berlin, Ger.)* **2010**, *212*, 1−12.

(5) Ishikawa, M.; Hashimoto, K. alpha7 nicotinic acetylcholine receptor as a potential therapeutic target for schizophrenia. *Curr. Pharm. Des.* **2011**, *17*, 121−129.

(6) Parri, H. R.; Hernandez, C. M.; Dineley, K. T. Research update: alpha7 nicotinic acetylcholine receptor mechanisms in Alzheimer's disease. *Biochem. Pharmacol.* **2011**, *82*, 931−942.

(7) Albuquerque, E. X.; Pereira, E. F.; Alkondon, M.; Rogers, S. W. Mammalian nicotinic acetylcholine receptors: from structure to function. *Physiol. Rev.* **2009**, *89*, 73−120.

(8) Woodruff-Pak, D. S.; Gould, T. J. Neuronal nicotinic acetylcholine receptors: involvement in Alzheimer's disease and schizophrenia. *Behav. Cognit. Neurosci. Rev.* **2002**, *1*, 5−20.

(9) D'Hoedt, D.; Bertrand, D. Nicotinic acetylcholine receptors: an overview on drug discovery. *Expert Opin. Ther. Targets* **2009**, *13*, 395−411.

(10) Hoffmeister, P. G.; Donat, C. K.; Schuhmann, M. U.; Voigt, C.; Walter, B.; Nieber, K.; Meixensberger, J.; Bauer, R.; Brust, P. Traumatic brain injury elicits similar alterations in alpha7 nicotinic receptor density in two different experimental models. *NeuroMol. Med.* **2011**, *13*, 44−53.

(11) Verbois, S. L.; Sullivan, P. G.; Scheff, S. W.; Pauly, J. R. Traumatic brain injury reduces hippocampal alpha7 nicotinic cholinergic receptor binding. *J. Neurotrauma* **2000**, *17*, 1001−1011.

(12) Verbois, S. L.; Scheff, S. W.; Pauly, J. R. Time-dependent changes in rat brain cholinergic receptor expression after experimental brain injury. *J. Neurotrauma* **2002**, *19*, 1569−1585.

(13) Olincy, A.; Harris, J. G.; Johnson, L. L.; Pender, V.; Kongs, S.; Allensworth, D.; Ellis, J.; Zerbe, G. O.; Leonard, S.; Stevens, K. E.; Stevens, J. O.; Martin, L.; Adler, L. E.; Soti, F.; Kem, W. R.; Freedman, R. Proof-of-concept trial of an alpha7 nicotinic agonist in schizophrenia. *Arch. Gen. Psychiatry* **2006**, *63*, 630−638.

(14) Thomsen, M. S.; Hansen, H. H.; Timmerman, D. B.; Mikkelsen, J. D. Cognitive improvement by activation of alpha7 nicotinic acetylcholine receptors: from animal models to human pathophysiology. *Curr. Pharm. Des.* **2010**, *16*, 323−343.

(15) Mazurov, A. A.; Speake, J. D.; Yohannes, D. Discovery and development of alpha7 nicotinic acetylcholine receptor modulators. *J. Med. Chem.* **2011**, *54*, 7943−7961.

(16) Taly, A.; Charon, S. alpha7 nicotinic acetylcholine receptors: a therapeutic target in the structure era. *Curr. Drug Targets* **2012**, *13*, 695−706.

(17) Wallace, T. L.; Bertrand, D. Alpha7 neuronal nicotinic receptors as a drug target in schizophrenia. *Expert Opin. Ther. Targets* **2013**, *17*, 139−155.

(18) Pomper, M. G.; Phillips, E.; Fan, H.; McCarthy, D. J.; Keith, R. A.; Gordon, J. C.; Scheffel, U.; Dannals, R. F.; Musachio, J. L. Synthesis and biodistribution of radiolabeled alpha 7 nicotinic acetylcholine receptor ligands. *J. Nucl. Med.* **2005**, *46*, 326−334.

(19) Hashimoto, K.; Nishiyama, S.; Ohba, H.; Matsuo, M.; Kobashi, T.; Takahagi, M.; Iyo, M.; Kitashoji, T.; Tsukada, H. [^{11}C]CHIBA-1001 as a novel PET ligand for alpha7 nicotinic receptors in the brain: a PET study in conscious monkeys. *PLoS One* **2008**, *3*, e3231.

(20) Ogawa, M.; Nishiyama, S.; Tsukada, H.; Hatano, K.; Fuchigami, T.; Yamaguchi, H.; Matsushima, Y.; Ito, K.; Magata, Y. Synthesis and evaluation of new imaging agent for central nicotinic acetylcholine receptor alpha7 subtype. *Nucl. Med. Biol.* **2010**, *37*, 347−355.

(21) Dolle, F.; Valette, H.; Hinnen, F.; Vaufrey, F.; Demphel, S.; Coulon, C.; Ottaviani, M.; Bottlaender, M.; Crouzel, C. Synthesis and preliminary evaluation of a carbon-11-labelled agonist of the α7 nicotinic acetylcholine receptor. *J. Labelled Compd. Radiopharm.* **2001**, *44*, 785−795.

(22) Toyohara, J.; Ishiwata, K.; Sakata, M.; Wu, J.; Nishiyama, S.; Tsukada, H.; Hashimoto, K. In vivo evaluation of alpha7 nicotinic acetylcholine receptor agonists [^{11}C]A-582941 and [^{11}C]A-844606 in mice and conscious monkeys. *PLoS One* **2010**, *5*, e8961.
(23) Horti, A. G.; Ravert, H. T.; Gao, Y.; Holt, D. P.; Bunnelle, W. H.; Schrimpf, M. R.; Li, T.; Ji, J.; Valentine, H.; Scheffel, U.; Kuwabara, H.; Wong, D. F.; Dannals, R. F. Synthesis and evaluation of new radioligands [^{11}C]A-833834 and [^{11}C]A-752274 for positron-emission tomography of alpha7-nicotinic acetylcholine receptors. *Nucl. Med. Biol.* **2013**, *40*, 395−402.
(24) Gao, Y.; Ravert, H. T.; Valentine, H.; Scheffel, U.; Finley, P.; Wong, D. F.; Dannals, R. F.; Horti, A. G. 5-(5-(6-[(11)C]methyl-3,6-diazabicyclo[3.2.0]heptan-3-yl)pyridin-2-yl)-1*H*-indole as a potential PET radioligand for imaging cerebral alpha7-nAChR in mice. *Bioorg. Med. Chem.* **2012**, *20*, 3698−3702.
(25) Toyohara, J.; Sakata, M.; Wu, J.; Ishikawa, M.; Oda, K.; Ishii, K.; Iyo, M.; Hashimoto, K.; Ishiwata, K. Preclinical and the first clinical studies on [^{11}C]CHIBA-1001 for mapping alpha7 nicotinic receptors by positron emission tomography. *Ann. Nucl. Med.* **2009**, *23*, 301−309.
(26) Ettrup, A.; Mikkelsen, J. D.; Lehel, S.; Madsen, J.; Nielsen, E. O.; Palner, M.; Timmermann, D. B.; Peters, D.; Knudsen, G. M. ^{11}C-NS14492 as a novel PET radioligand for imaging cerebral alpha7 nicotinic acetylcholine receptors: in vivo evaluation and drug occupancy measurements. *J. Nucl. Med.* **2011**, *52*, 1449−1456.
(27) Ravert, H. T.; Dorff, P.; Foss, C. A.; Mease, R. C.; Fan, H.; Holmquist, C. R.; Phillips, E.; McCarthy, D. J.; Heys, J. R.; Holt, D. P.; Wang, Y.; Endres, C. J.; Dannals, R. F.; Pomper, M. G. Radiochemical synthesis and in vivo evaluation of [^{18}F]AZ11637326: an agonist probe for the alpha7 nicotinic acetylcholine receptor. *Nucl. Med. Biol.* **2013**, *40*, 731−739.
(28) Rotering, S.; Scheunemann, M.; Fischer, S.; Hiller, A.; Peters, D.; Deuther-Conrad, W.; Brust, P. Radiosynthesis and first evaluation in mice of [^{18}F]NS14490 for molecular imaging of alpha7 nicotinic acetylcholine receptors. *Bioorg. Med. Chem.* **2013**, *21*, 2635−2642.
(29) Deuther-Conrad, W.; Fischer, S.; Hiller, A.; Becker, G.; Cumming, P.; Xiong, G.; Funke, U.; Sabri, O.; Peters, D.; Brust, P. Assessment of alpha7 nicotinic acetylcholine receptor availability in juvenile pig brain with [^{18}F]NS10743. *Eur. J. Nucl. Med. Mol. Imaging* **2011**, *38*, 1541−1549.
(30) Horti, A. G.; Villemagne, V. L. The quest for Eldorado: development of radioligands for in vivo imaging of nicotinic acetylcholine receptors in human brain. *Curr. Pharm. Des.* **2006**, *12*, 3877−3900.
(31) Toyohara, J.; Wu, J.; Hashimoto, K. Recent development of radioligands for imaging alpha7 nicotinic acetylcholine receptors in the brain. *Curr. Top. Med. Chem.* **2010**, *10*, 1544−1557.
(32) Brust, P.; Peters, D.; Deuther-Conrad, W. Development of radioligands for the imaging of alpha7 nicotinic acetylcholine receptors with positron emission tomography. *Curr. Drug Targets* **2012**, *13*, 594−601.
(33) Marutle, A.; Zhang, X.; Court, J.; Piggott, M.; Johnson, M.; Perry, R.; Perry, E.; Nordberg, A. Laminar distribution of nicotinic receptor subtypes in cortical regions in schizophrenia. *J. Chem. Neuroanat.* **2001**, *22*, 115−126.
(34) Kulak, J. M.; Schneider, J. S. Differences in alpha7 nicotinic acetylcholine receptor binding in motor symptomatic and asymptomatic MPTP-treated monkeys. *Brain Res.* **2004**, *999*, 193−202.
(35) Kulak, J. M.; Carroll, F. I.; Schneider, J. S. [^{125}I]-Iodomethyllycaconitine binds to alpha7 nicotinic acetylcholine receptors in monkey brain. *Eur. J. Neurosci.* **2006**, *23*, 2604−2610.
(36) Zhang, L.; Villalobos, A.; Beck, E. M.; Bocan, T.; Chappie, T. A.; Chen, L.; Grimwood, S.; Heck, S. D.; Helal, C. J.; Hou, X.; Humphrey, J. M.; Lu, J.; Skaddan, M. B.; McCarthy, T. J.; Verhoest, P. R.; Wager, T. T.; Zasadny, K. Design and selection parameters to accelerate the discovery of novel central nervous system positron emission tomography (PET) ligands and their application in the development of a novel phosphodiesterase 2A PET ligand. *J. Med. Chem.* **2013**, *56*, 4568−4579.
(37) Eckelman, W. C.; Reba, R. C.; Gibson, R. E. Receptor-binding radiotracers: a class of potential radiopharmaceuticals. *J. Nucl. Med.* **1979**, *20*, 350−357.
(38) Tanibuchi, Y.; Wu, J.; Toyohara, J.; Fujita, Y.; Iyo, M.; Hashimoto, K. Characterization of [^{3}H]CHIBA-1001 binding to alpha7 nicotinic acetylcholine receptors in the brain from rat, monkey, and human. *Brain Res.* **2010**, *1348*, 200−208.
(39) Ding, M.; Ghanekar, S.; Elmore, C. S.; Zysk, J. R.; Werkheiser, J. L.; Lee, C. M.; Liu, J.; Chhajlani, V.; Maier, D. L. [^{3}H]Chiba-1001 (methyl-SSR180711) has low in vitro binding affinity and poor in vivo selectivity to nicotinic alpha-7 receptor in rodent brain. *Synapse* **2012**, *66*, 315−322.
(40) Maier, D. L.; Hill, G.; Ding, M.; Tuke, D.; Einstein, E.; Gurley, D.; Gordon, J. C.; Bock, M. J.; Smith, J. S.; Bialecki, R.; Eisman, M.; Elmore, C. S.; Werkheiser, J. L. Pre-clinical validation of a novel alpha-7 nicotinic receptor radiotracer, [^{3}H]AZ11637326: target localization, biodistribution and ligand occupancy in the rat brain. *Neuropharmacology* **2011**, *61*, 161−171.
(41) Innis, R. B.; Cunningham, V. J.; Delforge, J.; Fujita, M.; Gjedde, A.; Gunn, R. N.; Holden, J.; Houle, S.; Huang, S. C.; Ichise, M.; Iida, H.; Ito, H.; Kimura, Y.; Koeppe, R. A.; Knudsen, G. M.; Knuuti, J.; Lammertsma, A. A.; Laruelle, M.; Logan, J.; Maguire, R. P.; Mintun, M. A.; Morris, E. D.; Parsey, R.; Price, J. C.; Slifstein, M.; Sossi, V.; Suhara, T.; Votaw, J. R.; Wong, D. F.; Carson, R. E. Consensus nomenclature for in vivo imaging of reversibly binding radioligands. *J. Cereb. Blood Flow Metab.* **2007**, *27*, 1533−1539.
(42) Tichauer, K. M.; Samkoe, K. S.; Sexton, K. J.; Hextrum, S. K.; Yang, H. H.; Klubben, W. S.; Gunn, J. R.; Hasan, T.; Pogue, B. W. In vivo quantification of tumor receptor binding potential with dual-reporter molecular imaging. *Mol. Imaging Biol.* **2011**, *14*, 584−592.
(43) Schrimpf, M. R.; Sippy, K. B.; Briggs, C. A.; Anderson, D. J.; Li, T.; Ji, J.; Frost, J. M.; Surowy, C. S.; Bunnelle, W. H.; Gopalakrishnan, M.; Meyer, M. D. SAR of alpha7 nicotinic receptor agonists derived from tilorone: exploration of a novel nicotinic pharmacophore. *Bioorg. Med. Chem. Lett.* **2012**, *22*, 1633−1638.
(44) Muller, K.; Faeh, C.; Diederich, F. Fluorine in pharmaceuticals: looking beyond intuition. *Science* **2007**, *317*, 1881−1886.
(45) Nag, M.; Jenks, W. S. Photochemistry of substituted dibenzothiophene oxides: the effect of trapping groups. *J. Org. Chem.* **2005**, *70*, 3458−3463.
(46) Manna, S.; Maity, S.; Rana, S.; Agasti, S.; Maiti, D. ipso-Nitration of arylboronic acids with bismuth nitrate and perdisulfate. *Org. Lett.* **2012**, *14*, 1736−1739.
(47) Smith, M. B.; March, J. *March's Advanced Organic Chemistry*; John Wiley & Sons, Inc.: Hoboken, NJ, 2007; pp 853−869.
(48) Kubinyi, H. The Quantitative Analysis of Structure−Activity Relationships. In *Burger's Medicinal Chemistry and Drug Discovery*; Wolff, M. E., Ed.; John Wiley & Sons: New York, 1995; pp 497−571.
(49) Miller, P. W.; Long, N. J.; Vilar, R.; Gee, A. D. Synthesis of ^{11}C, ^{18}F, ^{15}O, and ^{13}N radiolabels for positron emission tomography. *Angew. Chem., Int. Ed.* **2008**, *47*, 8998−9033.
(50) Hudlicky, M.; Pavlath, A. E. *Chemistry of Organic Fluorine Compounds II: A Critical Review*; Americal Chemical Society: Washington, DC, 1995; pp 286−289.
(51) Clark, J. H.; Wails, D. Fluorodenitration of activated diphenyl sulphones using tetramethylammonium fluoride. *J. Fluorine Chem.* **1995**, *70*, 201−205.
(52) Xiao, Y.; Abdrakhmanova, G. R.; Baydyuk, M.; Hernandez, S.; Kellar, K. J. Rat neuronal nicotinic acetylcholine receptors containing alpha7 subunit: pharmacological properties of ligand binding and function. *Acta Pharmacol. Sin.* **2009**, *30*, 842−850.
(53) Anderson, D. J.; Bunnelle, W.; Surber, B.; Du, J.; Surowy, C.; Tribollet, E.; Marguerat, A.; Bertrand, D.; Gopalakrishnan, M. [^{3}H]A-585539 [(1*S*,4*S*)-2,2-dimethyl-5-(6-phenylpyridazin-3-yl)-5-aza-2-azoniabicyclo[2.2.1]heptane], a novel high-affinity alpha7 neuronal nicotinic receptor agonist: radioligand binding characterization to rat and human brain. *J. Pharmacol. Exp. Ther.* **2008**, *324*, 179−187.
(54) Navarro, H. A.; Zhong, D.; Abrahm, P.; Xu, H.; Carroll, F. I. Synthesis and pharmacological characterization of ([^{125}I]-

iodomethyllycaconitine ([^{125}I]iodo-MLA). A new ligand for the α7 nicotinic acetylcholine receptor. *J. Med. Chem.* **2000**, *43*, 142−145.
(55) Xiao, Y.; Kellar, K. The comparative pharmacology and up-regulation of rat neuronal nicotinic receptor subtype binding sites stably expressed in transfected mammalian cells. *J. Pharmacol. Exp. Ther.* **2004**, *310*, 98−107.
(56) Clarke, P. B.; Schwartz, R. D.; Paul, S. M.; Pert, C. B.; Pert, A. Nicotinic binding in rat brain: autoradiographic comparison of [^{3}H]acetylcholine, [^{3}H]nicotine, and [^{125}I]-alpha-bungarotoxin. *J. Neurosci.* **1985**, *5*, 1307−1315.
(57) Whiteaker, P.; Davies, A. R.; Marks, M. J.; Blagbrough, I. S.; Potter, B. V.; Wolstenholme, A. J.; Collins, A. C.; Wonnacott, S. An autoradiographic study of the distribution of binding sites for the novel alpha7-selective nicotinic radioligand [^{3}H]-methyllycaconitine in the mouse brain. *Eur. J. Neurosci.* **1999**, *11*, 2689−96.
(58) Biton, B.; Bergis, O. E.; Galli, F.; Nedelec, A.; Lochead, A. W.; Jegham, S.; Godet, D.; Lanneau, C.; Santamaria, R.; Chesney, F.; Leonardon, J.; Granger, P.; Debono, M. W.; Bohme, G. A.; Sgard, F.; Besnard, F.; Graham, D.; Coste, A.; Oblin, A.; Curet, O.; Vige, X.; Voltz, C.; Rouquier, L.; Souilhac, J.; Santucci, V.; Gueudet, C.; Francon, D.; Steinberg, R.; Griebel, G.; Oury-Donat, F.; George, P.; Avenet, P.; Scatton, B. SSR180711, a novel selective alpha7 nicotinic receptor partial agonist: (1) binding and functional profile. *Neuropsychopharmacology* **2007**, *32*, 1−16.
(59) Hashimoto, K.; Ishima, T.; Fujita, Y.; Matsuo, M.; Kobashi, T.; Takahagi, M.; Tsukada, H.; Iyo, M. Phencyclidine-induced cognitive deficits in mice are improved by subsequent subchronic administration of the novel selective alpha7 nicotinic receptor agonist SSR180711. *Biol. Psychiatry* **2008**, *63*, 92−97.
(60) Pichat, P.; Bergis, O. E.; Terranova, J. P.; Urani, A.; Duarte, C.; Santucci, V.; Gueudet, C.; Voltz, C.; Steinberg, R.; Stemmelin, J.; Oury-Donat, F.; Avenet, P.; Griebel, G.; Scatton, B. SSR180711, a novel selective alpha7 nicotinic receptor partial agonist: (II) efficacy in experimental models predictive of activity against cognitive symptoms of schizophrenia. *Neuropsychopharmacology* **2007**, *32*, 17−34.
(61) Rollema, H.; Shrikhande, A.; Ward, K. M.; Tingley, F. D., 3rd; Coe, J. W.; O'Neill, B. T.; Tseng, E.; Wang, E. Q.; Mather, R. J.; Hurst, R. S.; Williams, K. E.; de Vries, M.; Cremers, T.; Bertrand, S.; Bertrand, D. Pre-clinical properties of the alpha4beta2 nicotinic acetylcholine receptor partial agonists varenicline, cytisine and dianicline translate to clinical efficacy for nicotine dependence. *Br. J. Pharmacol.* **2010**, *160*, 334−345.
(62) Mintun, M. A.; Raichle, M. E.; Kilbourn, M. R.; Wooten, G. F.; Welch, M. J. A quantitative model for the in vivo assessment of drug binding sites with positron emission tomography. *Ann. Neurol.* **1984**, *15*, 217−227.
(63) Meyer, E. M.; Kuryatov, A.; Gerzanich, V.; Lindstrom, J.; Papke, R. L. Analysis of 3-(4-hydroxy, 2-methoxybenzylidene)anabaseine selectivity and activity at human and rat alpha-7 nicotinic receptors. *J. Pharmacol. Exp. Ther.* **1998**, *287*, 918−925.